Inorg. Chem. **2006**, *45*, 1698–1713

Structural and Electronic Differences of Copper(I) Complexes with Tris(pyrazolyl)methane and Hydrotris(pyrazolyl)borate Ligands

Kiyoshi Fujisawa,*,† Tetsuya Ono,† Yoko Ishikawa,† Nagina Amir,† Yoshitaro Miyashita,† Ken-ichi Okamoto,† and Nicolai Lehnert*,‡

Graduate School of Pure and Applied Sciences, University of Tsukuba, Tsukuba 305-8571, Japan, and Institut für Anorganische Chemie, Christian-Albrechts-Universität, Olshausenstrasse 40, D-24098 Kiel, Germany

Received July 29, 2005

Copper(I) complexes with tripodal nitrogen-containing neutral ligands such as tris(3,5-diisopropyl-1-pyrazolyl)methane (L1′) and tris(3-tertiary-butyl-5-isopropyl-1-pyrazolyl)methane (L3′), and with corresponding anionic ligands such as hydrotris(3,5-diisopropyl-1-pyrazolyl)borate ($L1^-$) and hydrotris(3-tertiary-butyl-5-isopropyl-1-pyrazolyl)borate ($L3^-$) were synthesized and structurally characterized. Copper(I) complexes [Cu(L1′)Cl] (**1**), [Cu(L1′)($OClO_3$)] (**2**), [Cu(L1′)(NCMe)](PF_6) (**3a**), [Cu(L1′)(NCMe)](ClO_4) (**3b**), [Cu(L1′)(CO)](PF_6) (**4a**), and [Cu(L1′)(CO)](ClO_4) (**4b**) were prepared using the ligand L1′. Copper(I) complexes [Cu(L3′)Cl] (**5**) and [Cu(L3′)(NCMe)](PF_6) (**6**) with the ligand L3′ were also synthesized. Copper(I) complexes [Cu(L1)(NCMe)] (**7**) and [Cu(L1)(CO)] (**8**) were prepared using the anionic ligand $L1^-$. Finally, copper(I) complexes with anionic ligand $L3^-$ and acetonitrile (**9**) and carbon monoxide (**10**) were synthesized. The complexes obtained were fully characterized by IR, far-IR, ^{1}H NMR, and ^{13}C NMR spectroscopy. The structures of both ligands, L1′ and L3′, and of complexes **1**, **2**, **3a**, **3b**, **4a**, **4b**, **5**, **6**, **7**, and **10** were determined by X-ray crystallography. The effects of the differences in (a) the fourth ligand and the counteranion, (b) the steric hindrance at the third position of the pyrazolyl rings, and most importantly, (c) the charge of the N3 type ligands, on the structures, spectroscopic properties, and reactivities of the copper(I) complexes are discussed. The observed differences in the reactivities toward O_2 of the copper(I) acetonitrile complexes are traced back to differences in the oxidation potentials determined by cyclic voltammetry. A special focus is set on the carbonyl complexes, where the ^{13}C NMR and vibrational data are presented. Density functional theory (DFT) calculations are used to shed light on the differences in CO bonding in the compounds with neutral and anionic N3 ligands. In correlation with the vibrational and electrochemical data of these complexes, it is demonstrated that the C–O stretching vibration is a sensitive probe for the "electron richness" of copper(I) in these compounds.

Introduction

Copper as well as iron active sites dominate the field of biological oxygen activation and play an important role in homogeneous and heterogeneous catalysis. During the past decades, the structures and functions of copper proteins have been elucidated, and these results have been recognized as one of the most remarkable advances in biochemistry and bioinorganic chemistry.[1−4] The reactions of copper(I) complexes with O_2 and the oxidative properties of the resulting Cu_n/O_2 ($n = 1-3$) complexes have attracted much interest because of their relevance for biochemical systems[1−4] and potential applications to synthetic catalysis.[5−7] Although a

* To whom correspondence should be addressed. Phone: +81 29 853 6922. Fax: +81 29 853 6503. E-mail: kiyoshif@chem.tsukuba.ac.jp (K.F.). Phone: +49 431 880 1739. Fax: +49 431 880 1520. E-mail: nlehnert@ac.uni-kiel.de (N.L.).

† University of Tsukuba.

‡ Christian-Albrechts-Universität Kiel.

(1) (a) Sykes, A. G. *Struct. Bonding (Berlin)* **1990**, *75*, 175. (b) Adman, E. T. *Adv. Protein Chem.* **1992**, *42*, 145. (c) *Bioinorganic Chemistry of Copper*; Karlin, K. D., Tyeklár, Z., Eds.; Chapman & Hall: New York, 1993. (d) Holm, R. H.; Kennepohl, P.; Solomon, E. I. *Chem. Rev.* **1996**, *96*, 2239. (e) Kaim, W.; Rall, J. *Angew. Chem., Int. Ed. Engl.* **1996**, *35*, 43. (f) Messerschmidt, A. *Struct. Bonding (Berlin)* **1998**, *90*, 37. (g) Solomon, E. I.; Chen, P.; Metz, M.; Lee, S.-K.; Palmer, A. E. *Angew. Chem., Int. Ed.* **2001**, *40*, 4570.

(2) (a) *Handbook of Metalloproteins*; Messerschmidt, A.; Huber, R., Poulos, T., Wieghardt, K., Eds.; John Wiley & Sons: Chichester, U.K., 2001. (b) *Handbook on Metalloproteins*; Bertini, I., Sigel, A., Sigel, H. Eds.; Marcel Dekker: New York, 2001.

(3) (a) Solomon, E. I.; Szilagyi, R. K.; Geroge, S. D.; Basumallick, L. *Chem. Rev.* **2004**, *104*, 419. (b) Kuchar, J.; Hausinger, R. P. *Chem. Rev.* **2004**, *104*, 509.

10.1021/ic051290t CCC: $33.50
Published on Web 01/17/2006

Chart 1. Structures of the Ligands Covered in This Work: Hydrotris(3,5-diisopropylpyrazolyl)borate Anion ($L1^-$), Tris(3,5-diisopropylpyrazolyl)methane (L1′), Hydrotris(3-tertiary-butyl-5-isopropylpyrazolyl)borate Anion ($L3^-$), Tris(3-tertiary-butyl-5-isopropylpyrazolyl)methane (L3′), and Hydrotris(3,5-diphenylpyrazolyl)borate Anion ($L5^-$)[25]

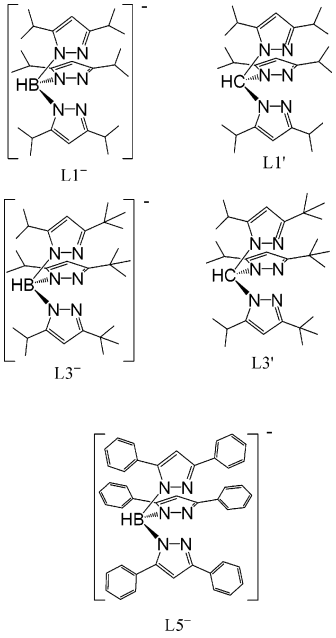

number of Cu_n/O_2 complexes have been reported, little research on the active sites of the copper(I)-containing proteins has appeared because of the featureless spectroscopic properties of the copper(I) centers. This is the result of the filled d^{10} electron configuration of the copper(I) ion, and therefore, it is difficult to detect copper(I) species by visible absorption spectroscopy. In addition, these sites are EPR silent. The structures of some copper(I)-containing proteins were obtained by X-ray structural analysis or NMR spectroscopy.[2] In these structures, N_2S or N_3 ligand donor sets coordinate to the copper(I) centers. Therefore, we use N_3 tripodal ligands such as hydrotris(pyrazolyl)borate anionic ligands or tris(pyrazolyl)methane neutral ligands to investigate these colorless compounds (Chart 1).

Hydrotris(pyrazolyl)borates ("borate" ligands), which can coordinate by three nitrogen atoms with tripod formation, are some of the most extensively studied ligands for coordination compounds in inorganic, bioinorganic, and coordination chemistry.[8] These borate ligands have a total charge of minus one. Their pyrazolyl ring arms can introduce many kinds of bulky substituents, especially at the third and fifth positions of the pyrazolyl rings. These include methyl, isopropyl, *tert*-butyl, phenyl, adamantyl, and other substituents.[9] The effective steric bulkiness for alkyl substituents as experienced by the metal center is summarized in eq 1.[10]

$$\text{Ad} > t\text{Bu} > i\text{Pr} > (\text{Ph}) > \text{Me} > \text{H} \qquad (1)$$

The following copper(I) carbonyl complexes were structurally characterized using these borate ligands: [Cu{HB(pz)$_3$}(CO)],[11,12] [Cu{HB(3,5-*i*Pr$_2$pz)$_3$}(CO)],[13−15] [Cu{HB(3,5-Ph$_2$pz)$_3$}(CO)],[13−15] [Cu{HB(3-*t*Bu-5-Mepz)$_3$}(CO)],[15,16] [Cu{HB(3,5-(CF$_3$)$_2$pz)$_3$}(CO)],[17] [Cu{HB(3-CF$_3$pz)$_3$}(CO)],[18] [Cu{HB(3-C$_2$F$_5$pz)$_3$}(CO)],[19] and [Cu{HB(3-C$_3$F$_7$pz)$_3$}(CO)].[20] On the other hand, the related tris(pyrazolyl)methanes ("methane" ligands), which have a framework identical to that of the borate ligands, contain a carbon atom in place of the boron atom and hence act as neutral ligands. The structures of the following copper(I) carbonyl and acetonitrile complexes with these methane ligands were reported: [Cu{HC(3-*t*Bupz)$_3$}(CO)](PF$_6$) and [Cu{HC(3-*t*Bupz)$_3$}(NCMe)](PF$_6$).[20] Comparison of the free borate and methane ligands and of corresponding complexes shows how the hindrance of the pyrazolyl substituents and especially the overall charge of the complexes controls the structures

(4) (a) Klinman, J. P. *Chem. Rev.* **1996**, *96*, 2541. (b) Solomon, E. I.; Sundaram, U. M.; Machonkin, T. E. *Chem. Rev.* **1996**, *96*, 2563. (c) Ferguson-Miller, S.; Babcock, G. T. *Chem. Rev.* **1996**, *96*, 2889. (d) Averill, B. A. *Chem. Rev.* **1996**, *96*, 2951.
(5) (a) Collman, J. P.; Boulatov, R.; Sunderland, C. J.; Fu, L. *Chem. Rev.* **2004**, *104*, 561. (b) Rorabacher, D. B. *Chem. Rev.* **2004**, *104*, 651. (c) Henkel, G.; Krebs, B. *Chem. Rev.* **2004**, *104*, 801. (d) Mirica, L. M.; Ottenwaelder, X.; Stack, T. D. P. *Chem. Rev.* **2004**, *104*, 1013. (e) Lewis, E. A.; Tolman, W. B. *Chem. Rev.* **2004**, *104*, 1047. (f) Kim, E.; Chufán, E. E.; Kamaraj, K.; Karlin, K. D. *Chem. Rev.* **2004**, *104*, 1077.
(6) (a) Ito, M.; Fujisawa, K.; Kitajima, N.; Moro-oka, Y. *Oxygenases and Model Systems*; Funabiki, T., Ed.; Kluwer Academic Publishers: Dordrecht, The Netherlands, 1997. (b) Karlin, K. D.; Zuberbühler, A. D. *Bioinorganic Catalysis*, 2nd ed.; Reedijk, J., Bouwman, E., Eds.; Marcel Dekker: New York, 1999. (c) Blackman, A. G.; Tolman, W. B. *Struct. Bonding (Berlin)* **2000**, *97*, 179. (d) Que, L., Jr.; Tolman, W. B. *Angew. Chem., Int. Ed.* **2002**, *41*, 1114. (e) Stack, T. D. P. *Dalton Trans*. **2003**, 1881. (f) Zhang, C. X.; Liang, H.-C.; Humphreys, K. J.; Karlin, K. D. *Advances in Catalytic Activation of Dioxygen by Metal Complexes*; Simándi, L. I., Ed., Kluwer Academic Publishers: Dordrecht, The Netherlands, 2003.
(7) (a) Kitajima, N.; Moro-oka, Y. *Chem. Rev.* **1994**, *94*, 737. (b) Solomon, E. I.; Tuczek, F.; Root, D. E.; Brown, C. A. *Chem. Rev.* **1994**, *94*, 827.
(8) For a recent book and reviews: (a) Trofimenko, S. *Chem. Rev.* **1993**, *93*, 943. (b) Kitajima, N.; Tolman, W. B. *Prog. Inorg. Chem.* **1995**, *43*, 419. (c) Parkin, G. *Adv. Inorg. Chem.* **1995**, *42*, 291. (d) Trofimenko, S. *Scorpionates: The Coordination Chemistry of Polypyrazolylborate Ligands*; Imperial College Press: London, 1999. (e) Parkin, G. *Chem. Commun.* **2000**, 1971.
(9) (a) Fujisawa, K.; Kobayashi, T.; Fujita, K.; Kitajima, N.; Moro-oka, Y.; Miyashita, Y.; Yamada, Y.; Okamoto, K. *Bull. Chem. Soc. Jpn.* **2000**, *73*, 1797. (b) Fujisawa, K.; Miyashita, Y.; Yamada, Y.; Okamoto, K.; *Bull. Chem. Soc. Jpn.* **2001**, *74*, 1065. (c) Fujisawa, K.; Tada, N.; Ishikawa, Y.; Higashimura, H.; Miyashita, Y.; Okamoto, K. *Inorg. Chem. Commun.* **2004**, *7*, 209.
(10) The hindered 7-tertiary-butyl-indazol-2-yl-substituted hydrotris(pyrazolyl)borate ligand has been reported. Rheingold, A. L.; Liable-Sands, L. M.; Yap, G. P. A.; Trofimenko, S. *Chem. Commun.* **1996**, 1233.
(11) Bruce, M. I.; Ostazewski, A. P. P. *J. Chem. Soc., Dalton Trans.* **1973**, 2433.
(12) Churchill, M. R.; DeBoer, B. G.; Rotella, F. J.; Salah, O. M. A.; Bruce, M. I. *Inorg. Chem.* **1975**, *14*, 2051.
(13) Kitajima, N.; Fujisawa, K.; Fujimoto, C.; Moro-oka, *Chem. Lett.* **1989**, 421.
(14) (a) Kitajima, N.; Fujisawa, K.; Moro-oka, Y.; Toriumi, K. *J. Am. Chem. Soc.* **1989**, *111*, 8975. (b) Kitajima, N.; Fujisawa, K.; Fujimoto, C.; Moro-oka, Y.; Hashimoto, S.; Kitagawa, T.; Toriumi, K.; Tatsumi, K.; Nakamura, A. *J. Am. Chem. Soc.* **1992**, *114*, 1277.
(15) Imai, S.; Fujisawa, K.; Kobayashi, T.; Shirasawa, N.; Fujii, H.; Yoshimura, T.; Kitajima, N.; Moro-oka, Y. *Inorg. Chem.* **1998**, *37*, 3066.
(16) Kiani, S.; Long, J. R.; Stavropoulos, P. *Inorg. Chim. Acta* **1997**, *263*, 357.
(17) Dias, H. V. R.; Lu, H.-L. *Inorg. Chem.* **1995**, *34*, 5380.
(18) Dias, H. V. R.; Kim, H.-J.; Lu, H.-L.; Rajeshwar, K.; Tacconi, N. R.; Derecskei-Kovacs, A.; Marynick, D. S. *Organometallics* **1996**, *15*, 2994.
(19) Dias, H. V. R.; Kim, H.-J. *Organometallics* **1996**, *15*, 5374.
(20) Reger, D. L.; Collins, J. E.; Rheingold, A. L.; Liable-Sands, L. M. *Organometallics* **1996**, *15*, 2029.

and physicochemical properties of the systems. In fact, borate and methane ligands with identical side chains are expected to have different nucleophilicities because of their different overall charges. In this study, the syntheses of the following four-coordinate copper(I) complexes are reported: chloro (**1**), perchlorato (**2**), acetonitrile (**3a** and **3b**), and carbonyl (**4a** and **4b**) complexes with HC(3,5-*i*Pr_2pz)$_3$; chloro (**5**) and acetonitrile (**6**) complexes with HC(3-*t*Bu-5-*i*Prpz)$_3$; acetonitrile (**7**) and carbonyl (**8**) complexes with HB(3,5-*i*Pr_2pz)$_3^-$; and acetonitrile (**9**) and carbonyl (**10**) complexes with HB(3-*t*Bu-5-*i*Prpz)$_3^-$. These complexes are characterized by IR, far-IR, and NMR spectroscopy and by X-ray crystallography. These results provide insight into the properties of the different ligands employed (i.e., the influence of the steric hindrance of the substituents and of the total charge of the ligands on the structures and properties of the complexes). In addition, density functional theory (DFT) calculations are presented on the carbonyl complexes to explore the differences in CO bonding with neutral methane and anionic borate ligands in correlation to the obtained experimental data. Finally, the reactivities of the copper(I) complexes toward O_2, CO, and MeCN are compared in detail.

Experimental Section

Materials. Preparation and handling of all complexes was performed under an argon atmosphere using standard Schlenk tube techniques or in a VAC inert atmosphere glovebox containing argon gas. Dichloromethane and acetonitrile were distilled from phosphorus pentoxide and calcium hydride prior to use, respectively. Diethyl ether and heptane were carefully purified by refluxing/distilling under an argon atmosphere over sodium benzophenone ketyl.[21] Methanol and acetone were spectroscopic grade and were used after bubbling with argon gas. Anhydrous solvents (dichloromethane, acetone, acetonitrile, and tetrahydrofuran) and tetrakis(acetonitrile)copper(I) hexafluorophosphate were purchased from Aldrich Chemical Co., Inc. and stored in a glovebox. Copper(I) chloride, which was purchased from Wako Pure Chemical Ind. Ltd., was purified according to a published method.[14b] ^{13}C-enriched carbon monoxide was obtained from Cambridge Isotope Laboratories, Inc. NMR solvents were also purchased from Cambridge Isotope Laboratories, Inc. and were purified by standard techniques.[21] The autoclave (TVS-1, 300 mL) was purchased from Taiatsu Techno Corp. for ligand syntheses. Silica gel (silica gel 60, particle size 0.063−0.0200 μm) for ligand purifications was obtained from Merck KGaA. Other reagents are commercially available and were used without further purification. Potassium hydrotris(3,5-diisopropyl-1-pyrazolyl)borate (K{HB(3,5-*i*Pr_2pz)$_3$} = KL1),[13,14] potassium hydrotris(3-tertiary-butyl-5-isopropyl-1-pyrazolyl)borate (K{HB(3-*t*Bu-5-*i*Prpz)$_3$} = KL3),[15] potassium hydrotris(3,5-diphenyl-1-pyrazolyl)borate (K{HB(3,5-Ph_2pz)$_3$} = KL5),[13,14b] and [Cu{HB(3,5-Ph_2pz)$_3$}(CO)] ([Cu(L5)(CO)]) (**11**)[13,14b] were prepared by published methods. The synthesis and structure of [Cu{HB(3,5-*i*Pr_2pz)$_3$}(CO)] ([Cu(L1)(CO)]) (**8**) have been reported before;[13,14b] however, this compound was prepared here by a modified procedure. The preparation of [Cu{HB(3-*t*Bu-5-*i*Prpz)$_3$}(CO)] ([Cu(L3)(CO)]) (**10**) has also been previously reported,[15] but the crystal structure of this complex was not determined. In this study, **10** was prepared by a different procedure to obtain crystals suitable for X-ray analysis. ***Caution:*** *Although we have not encountered any problems, it is noted that the perchlorate salts of metal complexes with organic ligands are potentially explosive and should be handled only in small quantities with appropriate precautions.*

Instrumentation. IR and far-IR spectra were recorded on KBr pellets in the 4600−400 cm^{-1} region and on CsI pellets in the 650−100 cm^{-1} region using a JASCO FT/IR-550 spectrophotometer. Abbreviations used in the description of vibrational data are as follows: vs, very strong; s, strong; m, medium; w, weak. ^{1}H and ^{13}C NMR spectra were obtained on a Bruker AVANCE−600 NMR spectrometer or a Bruker AVANCE−500 NMR spectrometer at room temperature (296 K) unless stated otherwise. Chemical shifts were reported as δ values downfield from the internal standard tetramethylsilane. Electrochemical measurements were carried out under an argon atmosphere at room temperature in acetonitrile solutions with tetrabutylammonium perchlorate as a supporting electrolyte using a BAS CV-50W voltammetric analyzer. A nonaqueous Ag/AgCl electrode (BAS, RE−5) and a platinum wire were used as reference and auxiliary electrodes, respectively. A platinum disk was used for the working electrode with a 50 mV/s scan rate. The ferrocenium/ferrocene couple was measured under the same conditions to correct for the junction potentials both as an internal reference and as a separate solution. The measured potentials were corrected by assigning the ferrocenium/ferrocene couple a value of 78 mV vs Ag/AgCl (ΔE = 96 mV).[22] Low-temperature UV−vis spectra were recorded on an Otsuka Electronics MCPD-2000 system with an optical fiber attachment at −78 °C in the 300−1100 nm region. The elemental analyses (C, H, N) were performed by the Research Facility Center for Science and Technology or the Department of Chemistry at the University of Tsukuba.

Calculations. Spin-restricted DFT calculations using Becke's three-parameter hybrid functional with the correlation functional of Lee, Yang, and Parr (B3LYP[23]) were performed using the program package Gaussian 98.[24] The structures of the borate and methane models [Cu(L0)(CO)] (**1̃**; L0 = HB(3,5-Me_2pz)$_3^-$) and [Cu(L0′)(CO)]$^+$ (**2̃**; L0′ = HC(3,5-Me_2pz)$_3$) have been fully optimized using B3LYP/LanL2DZ. Vibrational frequencies were calculated for these models showing no imaginary frequencies. The LanL2DZ basis set applies Dunning/Huzinaga full double-ζ (D95)[25] basis functions on the first row and Los Alamos effective core potentials plus DZ functions on all other atoms.[26] In addition, the structures of the CO-free systems [Cu(L0)] and [Cu(L0′)]$^+$ were also fully optimized. These structures were then used to calculate

(21) Armarego, W. L. F.; Perrin, D. D. *Purification of Laboratory Chemicals*, 4th ed.; Butterworth-Heinemann: Oxford, U.K., 1997.

(22) Connelly, N. G.; Geiger, W. E. *Chem. Rev.* **1996**, *96*, 877.

(23) (a) Becke, A. D. *Phys. Rev. A* **1988**, *38*, 3098. (b) Becke, A. D. *J. Chem. Phys.* **1993**, *98*, 1372. (c) Becke, A. D. *J. Chem. Phys.* **1993**, *98*, 5648.

(24) Frisch, M. J.; Trucks, G. W.; Schlegel, H. B.; Scuseria, G. E.; Robb, M. A.; Cheeseman, J. R.; Zakrzewski, V. G.; Montgomery, J. A., Jr.; Stratmann, R. E.; Burant, J. C.; Dapprich, S.; Millam, J. M.; Daniels, A. D.; Kudin, K. N.; Strain, M. C.; Farkas, O.; Tomasi, J.; Barone, V.; Cossi, M.; Cammi, R.; Mennucci, B.; Pomelli, C.; Adamo, C.; Clifford, S.; Ochterski, J.; Petersson, G. A.; Ayala, P. Y.; Cui, Q.; Morokuma, K.; Salvador, P.; Dannenberg, J. J.; Malick, D. K.; Rabuck, A. D.; Raghavachari, K.; Foresman, J. B.; Cioslowski, J.; Ortiz, J. V.; Baboul, A. G.; Stefanov, B. B.; Liu, G.; Liashenko, A.; Piskorz, P.; Komaromi, I.; Gomperts, R.; Martin, R. L.; Fox, D. J.; Keith, T.; Al-Laham, M. A.; Peng, C. Y.; Nanayakkara, A.; Challacombe, M.; Gill, P. M. W.; Johnson, B.; Chen, W.; Wong, M. W.; Andres, J. L.; Gonzalez, C.: Head-Gordon, M.; Replogle, E. S.; Pople, J. A. *Gaussian 98*, revision A.11; Gaussian, Inc.: Pittsburgh, 2001.

(25) *Modern Theoretical Chemistry*; Dunning, T. H., Jr.; Hay, P. J.; Schaefer, H. F., III, Eds.; Plenum: New York, 1976.

(26) (a) Hay, P. J.; Wadt, W. R. *J. Chem. Phys.* **1985**, *82*, 270 and 299. (b) Wadt, W. R.; Hay, P. J. *J. Chem. Phys.* **1985**, *82*, 284.

the formation energies of the CO complexes following the reaction [Cu(L)] + CO → [Cu(L)(CO)]. Values of about −33 kcal/mol are obtained for both the L0 and L0′ complexes. Single point calculations using BP86/TZVP were also performed on these structures to obtain the MO diagrams of the CO complexes. For these calculations, the TZVP basis set[27] has been applied as implemented in Gaussian98. Orbitals were plotted using GaussView.

Preparation of Ligands. HC(3,5-*i*Pr$_2$pz)$_3$, Tris(3,5-diisopropyl-1-pyrazolyl)methane, L1′.[28] Chloroform (130 mL) was added to a mixture of 3,5-diisopropylpyrazole[13,14] (7.28 g, 48.0 mmol), potassium carbonate (13.3 g, 96.0 mmol), and tetrabutylammonium hydrogensulfate (2.01 g, 5.90 mmol), and the mixture was bubbled with argon for 15 min. This solution was then heated and gently refluxed for 3 days at ∼95 °C (inner temperature of the autoclave). During the reaction time, the color of the solution became dark red-orange. The mixture was allowed to cool to room temperature; then, the precipitate was filtered off using a Büchner funnel and washed with acetone. The filtrate was dried in vacuo. The remaining brown oil was dissolved in a 1:1 mixture of ether/hexane (30 mL). The solution was chromatographed on a silica gel column. The desired fractions were eluted using a 1:2 mixture of ether/hexane. The solvent was then removed under vacuum to yield a yellow powder. This material was dissolved in a small amount of acetonitrile, and it was allowed to stand overnight at −30 °C. Yellow crystals were obtained, filtered off, and dried under vacuum. Yield: 64% (4.78 g, 10.2 mmol). Anal. Calcd for $C_{28}H_{46}N_6$: C, 72.06; H, 9.93; N, 18.01. Found: C, 71.81; H, 9.61; N, 18.00. IR (KBr, cm^{-1}): 2960vs, 2927s, 2869s, 1553s, 1463s, 1380s, 1294s, 1179m, 1081m, 995m, 905w, 837vs, 721w, 669w. ^{1}H NMR ($CDCl_3$, 600 MHz): δ 0.96 (d, J_{HH} = 6.8 Hz, 18H, CH(C*H*$_3$)), 1.18 (d, J_{HH} = 6.9 Hz, 18H, CH(C*H*$_3$)$_2$), 2.87 (sept, J_{HH} = 6.9 Hz, 3H, C*H*(CH$_3$)$_2$), 3.13 (sept, J_{HH} = 6.8 Hz, 3H, C*H*(CH$_3$)$_2$), 5.90 (s, 3H, 4-*H*(pz)), 8.27 (s, 1H, *H*C). ^{13}C NMR ($CDCl_3$, 150 MHz): δ 22.69 (CH(*C*H$_3$)$_2$), 23.04 (CH(*C*H$_3$)$_2$), 25.35 (*C*H(CH$_3$)$_2$), 27.88 (*C*H-(CH$_3$)$_2$), 80.16 (H*C*), 100.46 (pz-4*C*), 151.86 (pz-3*C*), 158.15 (pz-5*C*).

HC(3-*t*Bu-5-*i*Prpz)$_3$, Tris(3-tertiary-butyl-5-isopropyl-1-pyrazolyl)methane, L3′. L3′ was prepared in the same manner as L1 using chloroform (130 mL), 3-tertiary-butyl-5-isopropylpyrazole[15] (7.01 g, 42.1 mmol), potassium carbonate (8.97 g, 64.9 mmol), and tetrabutylammonium hydrogensulfate (2.02 g, 5.94 mmol). The filtrate was evaporated under vacuum, and a brown oil was obtained. Predried *p*-toluenesulfonic acid (0.103 g, 0.599 mmol) in toluene (100 mL) was then added to the remaining brown oil. The solution was heated and gently refluxed for 1 day at ∼138 °C (temperature of oil bath). The solution was allowed to cool to room temperature, and then it was evaporated under vacuum. The remaining brown oil was dissolved in a 1:2 mixture of ether/hexane (30 mL) and chromatographed on a silica gel column that was packed and flushed with a 1:5 ether/hexane solution. The fractions that contained the desired product were combined, and the solvent was removed under vacuum to yield a yellow powder. Recrystallization from acetonitrile at −30 °C gave colorless crystals. Single crystals were also obtained from acetonitrile at −30 °C. Yield: 49% (3.49 g, 6.86 mmol). Anal. Calcd for $C_{31}H_{52}N_6$: C, 73.18; H, 10.30; N, 16.52. Found: C, 73.30; H, 10.41; N, 16.29. IR (KBr, cm^{-1}): 2963vs, 2928m, 2867m, 1549m, 1485m, 1462m, 1362m, 1323m, 1308m, 1277w, 1232s, 1077w, 992w, 841m, 812m. ^{1}H NMR ($CDCl_3$, 600 MHz): δ 0.93 (d, J_{HH} = 6.8 Hz, 18H, CH(C*H*$_3$)$_2$), 1.21 (s, 27H, C(C*H*$_3$)$_3$), 3.19 (sept, J_{HH} = 6.8 Hz, 3H, C*H*(CH$_3$)$_2$), 5.90 (s, 3H, 4-*H*(pz)), 8.27 (s, 1H, *H*C). ^{13}C NMR ($CDCl_3$, 150 MHz): δ 23.5 (CH(*C*H$_3$)$_2$), 25.7 (*C*H(CH$_3$)$_2$), 30.8 (C(*C*H$_3$)$_3$), 32.4 (*C*(CH$_3$)$_3$), 80.5 (H*C*), 100.3 (4-*C*(pz)), 151.9 (3-*C*(pz)), 161.0 (5-*C*(pz)).

Preparation of Complexes. [Cu{HC(3,5-*i*Pr$_2$pz)$_3$}(Cl)], [Cu(L1′)Cl] (1). Acetone (80 mL) was added to a mixture of L1′ (1319 mg, 2.83 mmol) and copper(I) chloride (309 mg, 3.12 mmol) in a glovebox. After the mixture was stirred for 24 h, the solvent was evaporated under vacuum. The resulting solid was extracted with dichloromethane (60 mL). The filtrate was evaporated under vacuum and a yellowish white powder was obtained. Recrystallization from dichloromethane/ether at −30 °C gave colorless crystals. Yield: 82% (1304 mg, 2.31 mmol). Anal. Calcd for $C_{28}H_{46}N_6ClCu$: C, 59.45; H, 8.20; N, 14.86. Found: C, 59.19; H, 8.49; N, 15.11. IR (KBr, cm^{-1}): 2963vs, 1556vs, 1467vs, 1402s, 1382s, 1363m, 1290vs, 1233s, 1180s, 1108w, 1053s, 1005m, 913w, 823vs, 797s, 723w, 669m. Far-IR (CsI, cm^{-1}): 637m, 587m, 520s, 464w, 396s, 365w, 298vs, 176w, 154m. ^{1}H NMR (CD_2Cl_2, 600 MHz): δ 1.24 (d, J_{HH} = 6.3 Hz, 36H, CH(C*H*$_3$)$_2$), 3.03 (sept, J_{HH} = 6.8 Hz, 6H, C*H*(CH$_3$)$_2$), 5.98 (s, 3H, 4-*H*(pz)), 7.96 (s, 1H, *H*C). ^{13}C NMR (CD_2Cl_2, 150 MHz): δ 22.7 (CH(*C*H$_3$)$_2$), 23.3 (CH-(*C*H$_3$)$_2$), 26.5 (*C*H(CH$_3$)$_2$), 28.1 (*C*H(CH$_3$)$_2$), 69.8 (H*C*), 100.4 (4-*C*(pz)), 150.6 (3-*C*(pz)), 161.1 (5-*C*(pz)).

[Cu{HC(3,5-*i*Pr$_2$pz)$_3$}(OClO$_3$)], [Cu(L1′)(OClO$_3$)] (2). Dichloromethane (60 mL) and tetrahydrofuran (30 mL) were added to a mixture of [Cu(L1′)Cl] (**1**) (535 mg, 0.945 mmol) and silver perchlorate (243 mg, 1.17 mmol) in a glovebox. After the mixture was stirred for 1 h, the solvent was evaporated under vacuum. The resulting solid was extracted with dichloromethane (60 mL). The filtrate was evaporated under vacuum, and a greenish white powder was obtained. Recrystallization from dichloromethane/ether at −30 °C gave colorless crystals. Single crystals were obtained at room temperature. Yield: 65% (386 mg, 0.612 mmol). Anal. Calcd for $C_{28}H_{46}N_6ClCuO_4$: C, 53.41; H, 7.36; N, 13.35. Found: C, 53.20; H, 7.28; N, 13.19. IR (KBr, cm^{-1}): 2967vs, 2870m, 1556s, 1468s, 1400m, 1385m, 1365m, 1288s, 1262s, 1230s, 1182s, 1100vs, 1055vs, 1030vs, 908w, 871w, 821vs, 723w, 665m, 622m, 489w. Far-IR (CsI, cm^{-1}): 644w, 639w, 628vs, 619vs, 589w, 519s, 394s, 350w, 303m, 268m, 226s, 170w. ^{1}H NMR (CD_2Cl_2, 600 MHz): δ 1.23 (br, 18H, CH(C*H*$_3$)$_2$), 1.29 (d, J_{HH} = 6.6 Hz, 18H, CH(C*H*$_3$)$_2$), 3.07 (sept, J_{HH} = 6.7 Hz, 3H, C*H*(CH$_3$)$_2$), 3.20 (br, 3H, C*H*(CH$_3$)$_2$), 6.01 (s, 3H, 4-*H*(pz)), 7.97 (s, 1H, *H*C). ^{13}C NMR (CD_2Cl_2, 150 MHz): δ 22.7 (CH(*C*H$_3$)$_2$), 23.3 (CH(*C*H$_3$)$_2$), 26.7 (*C*H(CH$_3$)$_2$), 28.2 (*C*H(CH$_3$)$_2$), 67.8 (H*C*), 100.3 (4-*C*(pz)), 150.9 (3-*C*(pz)), 161.4 (5-*C*(pz)).

[Cu{HC(3,5-*i*Pr$_2$pz)$_3$}(NCMe)](PF$_6$), [Cu(L1′)(NCMe)](PF$_6$) (3a). The preparation was carried out in the same manner as that for **1** using L1′ (1271 mg, 2.72 mmol) in dichloromethane (30 mL) and tetrakis(acetonitrile)copper(I) hexafluorophosphate (1106 mg, 2.97 mmol) in acetonitrile (45 mL) in a glovebox. Recrystallization from dichloromethane/ether at −30 °C yielded colorless crystals. Single crystals were obtained from dichloromethane/ether at room temperature. Yield: 84% (1647 mg, 2.30 mmol). Anal. Calcd for $C_{30}H_{49}N_7CuF_6P$: C, 50.31; H, 6.90; N, 13.69. Found: C, 50.13; H, 6.68; N, 13.53. IR (KBr, cm^{-1}): 2971vs, 2872s, 1556s, 1470s, 1401s, 1386s, 1366m, 1291s, 1236s, 1183s, 1110w, 1061s, 1010m, 841vs, 738m, 669m, 558s. Far-IR (CsI, cm^{-1}): 634w, 621w, 560vs, 520m, 477s, 395m, 302m, 279w, 206s, 172w. ^{1}H NMR ($CDCl_3$, 600 MHz): δ 1.27 (d, J_{HH} = 7.0 Hz, 18H, CH(C*H*$_3$)$_2$), 1.31 (d, J_{HH} = 6.7 Hz, 18H, CH(C*H*$_3$)$_2$), 2.34 (s, 3H, C*H*$_3$CN), 3.03 (sept, J_{HH} = 7.0 Hz, 3H, C*H*(CH$_3$)$_2$), 3.25 (sept, J_{HH} = 6.7 Hz, 3H, C*H*(CH$_3$)$_2$), 5.96 (s, 3H, 4-*H*(pz)), 8.04 (s, 1H, *H*C). ^{13}C NMR ($CDCl_3$, 150 MHz): δ 19.8 (CH(*C*H$_3$)$_2$), 20.6 (CH(*C*H$_3$)$_2$), 23.4

(27) Schaefer, A.; Horn, H.; Ahlrichs, R. *J. Chem. Phys.* **1992**, *97*, 2571.
(28) Fujisawa, K.; Ono, T.; Aoki, H.; Ishikawa, Y.; Miyashita, Y.; Okamoto, K.; Nakazawa, H.; Higashimura, H. *Inorg. Chem. Commun.* **2004**, *7*, 330.

($CH(CH_3)_2$), 25.5 ($CH(CH_3)_2$), 64.4 (H*C*), 97.3 (4-*C*(pz)), 113.6 (CH_3CN), 148.9 (3-*C*(pz)), 158.0 (5-*C*(pz)).

[Cu{HC(3,5-*i*Pr$_2$pz)$_3$}(NCMe)](ClO$_4$), [Cu(L1′)(NCMe)](ClO$_4$) (3b). [Cu(L1′)($OClO_3$)] (**2**) (120 mg, 0.191 mmol) was dissolved in acetonitrile (15 mL) in a glovebox. After the mixture was stirred for 5 h, the solvent was evaporated under vacuum. The resulting solid was extracted with dichloromethane (5 mL). The filtrate was evaporated under vacuum, and a white powder was obtained. Recrystallization from dichloromethane/heptane at −50 °C produced colorless crystals. Yield: 46% (58.7 mg, 0.0875 mmol). Anal. Calcd for $C_{30}H_{49}N_7ClCuO_4$: C, 53.72; H, 7.36; N, 14.62. Found: C, 53.49; H, 7.44; N, 14.79. IR (KBr, cm^{-1}): 3132w, 2968vs, 2932s, 2871m, 1555s, 1469s, 1399m, 1385m, 1290s, 1233s, 1182m, 1097vs, 1009w, 915w, 822s, 624s. Far-IR (CsI, cm^{-1}): 624vs, 587m, 522s, 396s, 303m, 279w, 202m. ^{1}H NMR (CD_2Cl_2, 600 MHz): δ 1.18 (d, J_{HH} = 7.0 Hz, 18H, $CH(CH_3)_2$), 1.22 (d, J_{HH} = 6.8 Hz, 18H, $CH(CH_3)_2$), 2.29 (s, 3H, CH_3CN), 2.97 (sept, J_{HH} = 7.0 Hz, 3H, $CH(CH_3)_2$), 3.04 (sept, J_{HH} = 6.7 Hz, 3H, $CH(CH_3)_2$), 5.95 (s, 3H, 4-*H*(pz)), 7.89 (s, 1H, H*C*). ^{13}C NMR (CD_2Cl_2, 150 MHz): δ 22.2 ($CH(CH_3)_2$), 23.0 ($CH(CH_3)_2$), 26.3 ($CH(CH_3)_2$), 28.2 ($CH(CH_3)_2$), 67.3 (H*C*), 100.3 (4-*C*(pz)), 151.2 (3-*C*(pz)), 161.0 (5-*C*(pz)).

[Cu{HC(3,5-*i*Pr$_2$pz)$_3$}(CO)](PF$_6$), [Cu(L1′)(CO)](PF$_6$) (4a). [Cu(L1′)(NCMe)](PF_6) (**3a**) (133 mg, 0.186 mmol) was dissolved in dichloromethane (15 mL) in a glovebox. The solution was cooled to −78 °C in an argon atmosphere, and the argon was then replaced by CO. The solution was allowed to warm to room temperature. After the solution was stirred for 36 h, the solvent was evaporated under vacuum. The resulting solid was extracted with chloroform (10 mL). The filtrate was evaporated under vacuum, and a white powder was obtained. Recrystallization from chloroform/heptane at −30 °C gave colorless crystals. Yield: 22% (29.1 mg, 0.0414 mmol). Anal. Calcd for $C_{29}H_{46}N_6CuF_6OP$: C, 49.53; H, 6.59; N, 11.95. Found: C, 49.43; H, 6.63; N, 11.99. IR (KBr, cm^{-1}): 3139w, 2969s, 2935m, 2873w, 2109vs, 1556s, 1470s, 1401m, 1290s, 1234s, 1183m, 1107w, 1062m, 1015w, 844vs, 670m, 557s. Far-IR (CsI, cm^{-1}): 641w, 631w, 558vs, 524m, 449s, 396m, 302m, 291w, 280w, 211w, 166s. ^{1}H NMR ($CDCl_3$, 600 MHz): δ 1.31 (d, J_{HH} = 7.0 Hz, 18H, $CH(CH_3)_2$), 1.32 (d, J_{HH} = 6.7 Hz, 18H, $CH(CH_3)_2$), 3.00 (sept, J_{HH} = 7.0 Hz, 3H, $CH(CH_3)_2$), 3.45 (sept, J_{HH} = 6.7 Hz, 3H, $CH(CH_3)_2$), 6.04 (s, 3H, 4-*H*(pz)), 8.19 (s, 1H, H*C*). ^{13}C NMR ($CDCl_3$, 150 MHz): δ 22.5 ($CH(CH_3)_2$), 23.1 ($CH(CH_3)_2$), 25.6 ($CH(CH_3)_2$), 28.5 ($CH(CH_3)_2$), 66.9 (H*C*), 100.1 (4-*C*(pz)), 154.0 (3-*C*(pz)), 161.2 (5-*C*(pz)).

[Cu{HB(3,5-*i*Pr$_2$pz)$_3$}(NCMe)], [Cu(L1)(NCMe)] (7). A solution of KL1 (1324 mg, 2.62 mmol) in dichloromethane (30 mL) was added to a solution of tetrakis(acetonitrile)copper(I) hexafluorophosphate (1089 mg, 2.92 mmol) in acetonitrile (50 mL) in a glovebox. After the mixture was stirred for 1 h, the solvent was evaporated under vacuum. The resulting solid was extracted with dichloromethane (70 mL) and acetonitrile (70 mL). The filtrate was evaporated under vacuum, and a white powder was obtained. Recrystallization from acetonitrile at −30 °C yielded colorless crystals. Single crystals were obtained from dichloromethane/acetonitrile at 4 °C. Yield: 41% (620 mg, 1.09 mmol). Anal. Calcd for $C_{29}H_{49}N_7BCu$: C, 61.10; H, 8.66; N, 17.20. Found: C, 61.18; H, 8.90; N, 17.26. IR (KBr, cm^{-1}): 2957vs, 2526s, 2255m, 1534vs, 1460vs, 1380vs, 1297vs, 1173vs, 1135s, 1092m, 1042vs, 957w, 922w, 898m, 878w, 837w, 818m, 783vs, 757vs, 715s, 654vs, 586w, 515w. ^{1}H NMR (CD_2Cl_2, 600 MHz): δ 1.20 (d, J_{HH} = 6.8 Hz, 18H, $CH(CH_3)_2$), 1.25 (d, J_{HH} = 7.0 Hz, 18H, $CH(CH_3)_2$), 2.16 (s, 3H, CH_3CN), 3.06 (sept, J_{HH} = 7.0 Hz, 3H, $CH(CH_3)_2$), 3.44 (sept, J_{HH} = 6.7 Hz, 3H, $CH(CH_3)_2$), 5.75 (s, 3H, 4-*H*(pz)). ^{13}C NMR (CD_2Cl_2, 150 MHz): δ 20.0 ($CH(CH_3)_2$), 20.8 ($CH(CH_3)_2$), 23.3 ($CH(CH_3)_2$), 25.1 ($CH(CH_3)_2$), 93.3 (4-*C*(pz)), 122.1 (CH_3CN), 151.3 (3-*C*(pz)), 154.4 (5-*C*(pz)).

[Cu{HB(3,5-*i*Pr$_2$pz)$_3$}(CO)], [Cu(L1)(CO)] (8). The preparation was carried out in the same manner as for **4b** using [Cu(L1)(NCMe)] (**7**) (129 mg, 0.226 mmol) in dichloromethane (12 mL) with some modifications of the literature procedure.[13,14b,15]. Recrystallization from acetone at −30 °C gave colorless crystals. Yield: 54% (67.5 mg, 0.121 mmol). Anal. Calcd for $C_{28}H_{46}N_6BCuO$: C, 60.37; H, 8.32; N, 15.09. Found: C, 60.09; H, 8.21; N, 15.00. IR (KBr, cm^{-1}): 2957s, 2926m, 2862m, 2525w, 2056vs, 1534m, 1469m, 1397w, 1381m, 1300m, 1169m, 1046m, 786m. Far-IR (CsI, cm^{-1}): 624m, 580w, 520s, 466s, 398m, 291w, 268w, 212w, 175vs. ^{1}H NMR ($CDCl_3$, 600 MHz): δ 1.21 (d, J_{HH} = 6.9 Hz, 18H, $CH(CH_3)_2$), 1.25 (d, J_{HH} = 7.0 Hz, 18H, $CH(CH_3)_2$), 3.03 (sept, J_{HH} = 7.0 Hz, 3H, $CH(CH_3)_2$), 3.41 (sept, J_{HH} = 6.7 Hz, 3H, $CH(CH_3)_2$), 5.74 (s, 3H, 4-*H*(pz)). ^{13}C NMR ($CDCl_3$, 150 MHz): δ 23.1 ($CH(CH_3)_2$), 23.6 ($CH(CH_3)_2$), 26.0 ($CH(CH_3)_2$), 28.3 ($CH(CH_3)_2$), 96.3 (4-*C*(pz)), 154.4 (3-*C*(pz)), 157.4 (5-*C*(pz)).

The methods for the preparation of the complexes **4b**, **5**, **6**, **9**, and **10** are similar to those described above and are therefore given in the Supporting Information. ^{13}CO-labeled complexes were prepared using the same method as for the corresponding unlabeled complexes but with ^{13}CO gas.

Reaction of [Cu(L1′)($OClO_3$)] (2) with O_2. Complex **2** was dissolved in dichloromethane in a Schlenk tube and cooled to −78 °C in an argon atmosphere. The argon was then replaced with O_2, and the solution was stirred at −78 °C for 1 h. During this time, the color of the solution changed from colorless to deep purple. Quantitative formation of [{Cu(L1′)}$_2$(μ-O_2)](ClO_4)$_2$ was indicated by UV−vis spectroscopy.[29]

Reaction of [Cu(L1′)(NCMe)](PF_6) (3a)/[Cu(L1′)(NCMe)](ClO$_4$) (3b) with O_2. Complex **3a**/**3b** was dissolved in dichloromethane in a Schlenk tube and cooled to −78 °C in an argon atmosphere. The argon was then replaced by O_2, and the solution was stirred at −78 °C for 5.5 h. This solution was characterized by UV−vis spectroscopy after 5.5, 94.5, and 601 h at −78 °C. During this process, the color of the solution turned from colorless to pale purple. Altogether, a slow formation of the peroxo complex [{Cu(L1′)}(μ-O_2)](PF_6)$_2$/[{Cu(L1′)}(μ-O_2)](ClO_4)$_2$ was observed.[29] UV−vis (CH_2Cl_2, λ_{max}, nm (conversion, per mole)): **3a** 5.5 h 344 (0.2%), 100 h 344 (0.9%), 701 h 344 (3.7%); **3b** 5.5 h 344 (1.7%), 100 h 344 (3.9%), 701 h 344 (8.6%).

Reaction of [Cu(L1)(NCMe)] (7) with O_2. In a Schlenk tube, complex **7** was dissolved in dichloromethane, and the mixture was cooled to −78 °C in an argon atmosphere. The argon was replaced with O_2, and the solution was stirred at −78 °C for 1 h. During this process, the color of the solution changed from colorless to deep purple indicating almost quantitative formation of [{Cu(L1)}$_2$(μ-O_2)].[14]

Details of all additional reactions performed with O_2, CO, and MeCN discussed in the text (Schemes 2−3) are given in the Supporting Information.

X-ray Data Collection and Structural Determination. Crystal data and refinement parameters for the investigated ligands (L1′ and L3′) and complexes (**1**, **2**, **3a**, **3b**, **4a**, **4b**, **5**, **6**, **7**, and **10**) are given in Tables 1 and 2. The diffraction data for all complexes except **7** and **10** were measured on a Rigaku/MSC Mercury CCD system with graphite monochromated Mo Kα (λ = 0.71069 Å) radiation at 23 °C for L1′, L3′, and **4a**, at −61 °C for **1**, **2**, **3a**, **5**, and **6**, and at −70 °C for **3b** and **4b**. Each crystal was mounted on the tip of a glass fiber by heavy-weight oil. The unit cell parameters

(29) Fujisawa, K. Manuscript in preparation.

Table 1. Crystallographic Data of the Ligands L1′ and L3′ and the Copper(I) Complexes **1**, **2**, **3a**, and **3b**

	L1′	L3′	**1**·CH_2Cl_2	**2**	**3a**·CH_2Cl_2	**3b**·$3CH_2Cl_2$·H_2O
formula	$C_{28}H_{46}N_6$	$C_{31}H_{52}N_6$	$C_{29}H_{48}Cl_3CuN_6$	$C_{28}H_{46}ClCuN_6O_4$	$C_{31}H_{51}Cl_2CuF_6N_7P$	$C_{33}H_{57}Cl_7CuN_7O_5$
fw	466.71	508.79	650.64	629.71	801.21	943.57
cryst syst	monoclinic	monoclinic	triclinic	orthorhombic	orthorhombic	monoclinic
space group	$P2_1/n$ (No. 14)	$P2_1/a$ (No. 14)	$P\bar{1}$ (No. 2)	*Pbca* (No. 61)	*Pbca* (No. 61)	$P2_1/c$ (No. 14)
a (Å)	11.221(2)	11.777(2)	9.767(7)	18.333(9)	16.240(4)	13.589(6)
b (Å)	14.921(2)	22.315(4)	11.841(8)	15.787(8)	27.748(7)	21.247(10)
c (Å)	18.382(2)	12.774(2)	16.592(12)	22.395(11)	17.750(5)	16.155(8)
α (deg)	90	90	109.96(2)	90	90	90
β (deg)	106.571(6)	94.287(9)	96.35(3)	90	90	93.546(6)
γ (deg)	90	90	105.55(3)	90	90	90
V (Å^3)	2949.9(7)	3347.7(10)	1693.8(21)	6481.3(54)	7998.7(35)	4655.1(38)
Z	4	4	2	8	8	4
D_{calcd} (g cm^{-3})	1.051	1.009	1.276	1.291	1.331	1.346
μ(Mo Kα) (cm^{-1})	0.63	0.61	9.08	7.97	7.78	9.14
2θ range (deg)	6−55	6−55	6−55	6−55	6−55	6−55
reflns collected	24530	28195	13253	54229	66731	38683
unique reflns	6715	7657	7432	7381	9113	10592
R_{int}	0.047	0.098	0.037	0.074	0.050	0.066
no. of observations	3138 ($I > 3.5\sigma(I)$)	1942 ($I > 3.5\sigma(I)$)	6384 ($I > 3\ \sigma(I)$)	2095 ($I > 5\ \sigma(I)$)	5057 ($I > 3\ \sigma\ (I)$)	5820 ($I > 5\ \sigma(I)$)
no. of variables	353	386	400	407	484	533
Final *R*, R_w[a]	0.082, 0.074	0.089, 0.055	0.081, 0.116	0.095, 0.109	0.087, 0.080	0.091, 0.115
max/min peak (e Å^{-3})	0.42/−0.43	0.32/−0.26	0.78/−0.74	0.96/−0.55	0.82/−0.64	1.07/−0.89

[a] $R = \sum||F_o| - |F_c||/\sum|F_o|$; $R_w = [(\sum w(|F_o| - |F_c|)^2/\sum wF_o^2)]^{1/2}$, $w = 1/\sigma^2(|F_o|)$.

Table 2. Crystallographic Data of the Copper(I) Complexes **4a**, **4b**, **5**, **6**, **7**, and **10**

	4a	**4b**·$3CHCl_3$	**5**	**6**·$3CH_2Cl_2$	**7**·$2CH_3CN$·$3H_2O$	**10**
formula	$C_{29}H_{46}CuF_6N_6OP$	$C_{32}H_{49}Cl_{10}CuN_6O_5$	$C_{31}H_{52}ClCuN_6$	$C_{36}H_{60}Cl_6CuF_6N_7P$	$C_{33}H_{61}BCuN_9O_3$	$C_{31}H_{52}BCuN_6O$
fw	703.23	1015.85	607.79	1012.15	706.26	599.15
cryst syst	monoclinic	monoclinic	orthorhombic	orthorhombic	monoclinic	monoclinic
space group	$P2_1/n$ (No. 14)	$P2_1/n$ (No. 14)	*Pnma* (No. 62)	*Pnma* (No. 62)	*C*2/*c* (No. 15)	$P2_1/m$ (No. 11)
a (Å)	12.691(6)	15.8003(8)	19.985(9)	33.238(12)	36.99(1)	10.592(1)
b (Å)	16.815(7)	15.4502(7)	16.608(7)	15.422(6)	12.453(4)	17.145(1)
c (Å)	17.295(8)	19.3019(10)	9.847(5)	9.683(4)	21.097(6)	9.741(2)
α (deg)	90	90	90	90	90	90
β (deg)	100.862(5)	93.6570(9)	90	90	122.23(2)	104.20(1)
γ (deg)	90	90	90	90	90	90
V (Å^3)	3624.6(27)	4702.3(4)	3268.4(25)	4963.6(32)	8221(4)	1714.9(8)
Z	4	4	4	4	8	2
D_{calcd} (g cm^{-3})	1.289	1.435	1.235	1.354	1.141	1.160
μ(Mo Kα) (cm^{-1})	7.08	10.74	7.79	8.50	5.72	6.68
2θ range (deg)	8−55	8−55	8−55	8−55	3−45	5−48
reflns collected	30120	39573	27089	41104	5467	2941
unique reflns	8264	10650	3829	39271	5371	2766
R_{int}	0.044	0.040	0.055	0.044	0.029	0.015
no. of observations	4921 ($I > 3\sigma(I)$)	5540 ($I > 5\ \sigma(I)$)	2087 ($I > 4\ \sigma(I)$)	24926 ($I > 5\ \sigma(I)$)	3635 ($I > 2\ \sigma(I)$)	1650 ($I > 5\ \sigma(I)$)
no. of variables	443	536	225	323	415	199
Final *R*, R_w[a]	0.082, 0.080	0.056, 0.050	0.056, 0.060	0.081, 0.102	0.064, 0.077	0.068, 0.054
max/min peak (e Å^{-3})	0.78/−0.69	0.77/−1.07	0.56/−0.57	10.10/−7.17	0.47/−0.33	0.63/−0.95

[a] $R = \sum||F_o| - |F_c||/\sum|F_o|$; $R_w = [(\sum w(|F_o| - |F_c|)^2/\sum wF_o^2)]^{1/2}$, $w = 1/\sigma^2(|F_o|)$.

of each crystal from 6 image frames were retrieved using Rigaku Daemon software and refined using CrystalClear on all observed reflections.[30] Data using 0.5° intervals in ϕ and ω for 25 s/frame (L1′, L3′, **1**, and **3a**), for 30 s/frame (**2**, **3b**, and **4a**), for 40 s/frame (**4b**), for 35 s/frame (**5**), and for 20 s/frame (**6**) were collected with a maximum resolution of 0.77 Å (744 oscillation images). The highly redundant data sets were reduced using CrystalClear and corrected for Lorentz and polarization effects. An empirical absorption correction was applied for each complex.[30−32] Structures were solved by direct methods (SIR 92).[33] The positions of the metal atoms and their first coordination sphere were located from the *E* map; other non-hydrogen atoms were found in alternating difference Fourier syntheses.[34] Least-squares refinement cycles were refined anisotropically during the final cycles (CrystalStructure).[31,32] Hydrogen atoms were placed in calculated positions. The remaining strong peaks in **6** are from the disordered solvent.

The diffraction data were measured on a Rigaku AFC 7R for **7** (at 23 °C) and AFC 7S for **10** (at −59 °C), which are automated four-circle diffractometers with graphite monochromated Mo Kα ($\lambda = 0.71069$ Å) radiation. Crystals were mounted on glass fiber by epoxy glue. The unit cell parameters of each crystal were obtained from a least-squares refinement based on 20 reflections. Over the course of the data collection for **7**, the standards decreased

(30) *CrystalClear*, version 1.3. Pflugrath, J. W. *Acta Crystallogr., Sect. D* **1999**, *55*, 1718.
(31) *CrystalStructure*, version 3.51; Rigaku: The Woodlands, TX, 2003.
(32) *Crystal Issue 10*; Watkin, D. J., Prout, C. K., Carruthers, J. R., Betteridge, P. W., Eds.; Chemical Crystallography Laboratory: Oxford, UK, 1996.
(33) *SIR 92*. Altomare, A.; Cascarano, G.; Giacovazzo, C.; Guagliardi, A.; Burla, M.; Polidori, G.; Camalli, M. J. *Appl. Crystallogr.* **1994**, *27*, 435.
(34) Beurskens, P. T.; Admiraal, G.; Beurskens, G.; Bosman, W. P.; de Gelder, R.; Israel, R.; Smits, J. M. M. *DIRDIF-99*; Technical Report of the Crystallography Laboratory; University of Nijmegen: Nijmegen, The Netherlands, 1999.

Scheme 1. Schematic Drawings of Each Reaction Performed in This Work

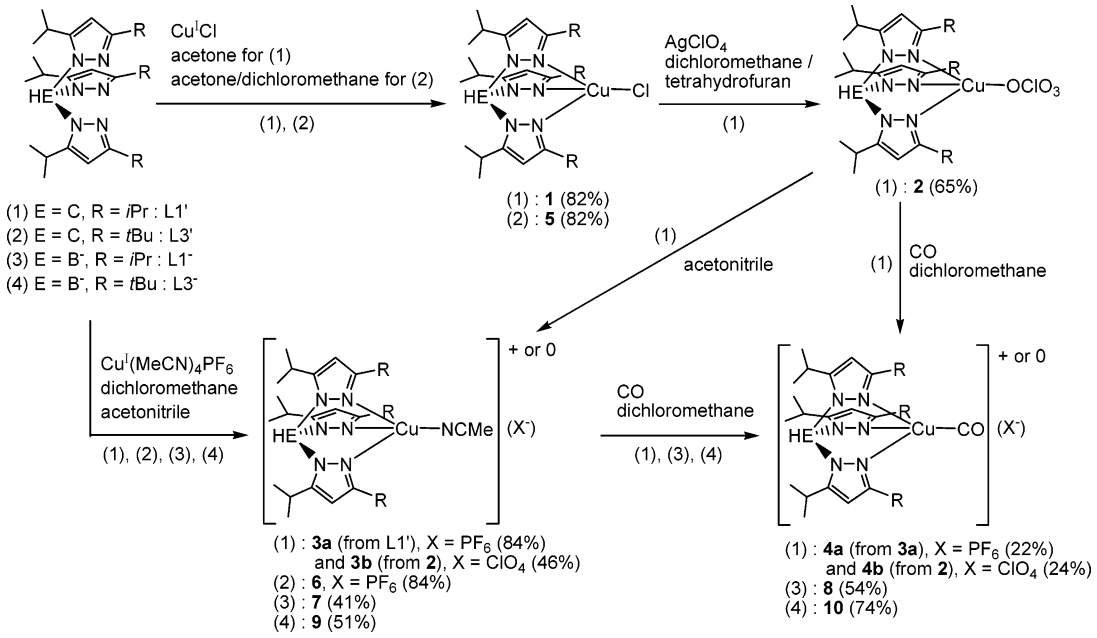

by 14.5%. Therefore, a linear correction factor was applied to the data to account for this phenomenon.[35] The intensity of three representative reflections monitored every 100 reflections did not show any decay for **10**. An empirical absorption correction was applied for **7** and **10**.[35] All data were corrected for Lorentz and polarization effects. The structures were solved by Patterson methods (PATTY)[36] for **7** and direct methods (MITHRIL 91)[37] for **10** and expanded using Fourier techniques.[38] Non-hydrogen atoms were refined anisotropically. Hydrogen atoms were located at calculated positions. Highly disordered O atoms of the water molecules in **7** were refined isotropically. Refinement was carried out by a full-matrix least-squares method on *F*. All calculations were performed using the teXsan crystallographic software package of the Molecular Structure Corporation.[35]

Results

Synthesis of Ligands. Trofimenko reported the synthesis of several tris(pyrazolyl)methane ligands and some transition metal compounds.[39] Eluguero and co-workers[40] and Reger and co-workers[41] have developed improved procedures for the synthesis of these N3 tripodal ligands. The preparation of the highly hindered 3,5-disubstituted tris(pyrazolyl)-methane ligands, L1′ and L3′, under solid−liquid phase transfer conditions using an autoclave was reported recently for the first time.[28] The reactions of 3,5-*i*Pr$_2$-pzH and 3-*t*Bu-5-*i*Pr-pzH with $CHCl_3$ in the presence of anhydrous potassium carbonate (base) and tetrabutylammonium hydrogensulfate (catalyst) were carried out as shown in eq 2 over 3 days for L1′ and over 15 days for L3′ at ∼95 °C (inner temperature of the autoclave), which was needed for the reaction to complete. As observed previously for the preparation of HC(3-Phpz)$_3$ and HC(3-*i*Prpz)$_3$, these pyrazole reactions yield a number of regioisomers, and hence, an isomerization reaction is needed in the case of L3′ to obtain the desired isomer. This was done in a toluene solution using anhydrous *p*-toluenesulfonic acid and refluxing the reaction mixture.[41]

$$\begin{array}{l}\text{3,5-diisopropylpyrazole} \\ \text{3-}\textit{tert}\text{-butyl-5-isopropylpyrazole}\end{array} \xrightarrow[CHCl_3]{(Bu_4N)HSO_4/Na_2CO_3} \text{L1′(64\%)}$$

$$\text{crude L3′} \xrightarrow[C_6H_5CH_3]{p\text{-toluenesulfonic acid}} \text{L3′(49\%)} \quad (2)$$

The related borate ligands, KL1, KL3, and KL5 were prepared in accordance to the literature but in higher yields.[13−15]

Syntheses of Complexes. All copper(I) complexes were prepared in a glovebox to avoid the reaction with O_2. Schematic drawings of all complex preparations performed in this work are summarized in Scheme 1. [Cu(L1′)Cl] (**1**), [Cu(L1′)($OClO_3$)] (**2**), [Cu(L1′)(NCMe)](PF_6) (**3a**), [Cu(L1′)-(NCMe)](ClO_4) (**3b**), [Cu(L1′)(CO)](PF_6) (**4a**), and [Cu(L1′)-(CO)](ClO_4) (**4b**) were prepared using ligand L1′. Complexes **1** and **3a** were obtained from L1′ and the corresponding copper(I) salts. Complex **2** was synthesized via the reaction of **1** with silver perchlorate. Complex **3b** was obtained from the reaction of **2** with MeCN. Interestingly, complexes **3a** and **3b** are relatively stable toward O_2 in contrast to **2** in

(35) *teXsan: Single-Crystal Structure Analysis Package*, version 1.10b; Molecular Structure Corporation: The Woodlands, TX, 1999.
(36) Beurskens, P. T.; Admiraal, G.; Beurskens, G.; Bosman, W. P.; Garcia-Granda, S.; Gould, R. O.; Smits, J. M. M.; Smykalla, C. *PATTY*; Technical Report of the Crystallography Laboratory; University of Nijmegen: Nijmegen The Netherlands.
(37) Gilmore, C. J. *MITHRIL: An Integrated Direct Methods Computer Program*; University of Glasgow: Glasgow, Scotland, 1990.
(38) Beurskens, P. T.; Admiraal, G.; Beurskens, G.; Bosman, W. P.; de Gelder, R.; Israel, R.; Smits, J. M. M. *DIRDIF-94*; Technical Report of the Crystallography Laboratory; University of Nijmegen: Nijmegen, The Netherlands, 1994.
(39) Trofimenko, S. *J. Am. Chem. Soc.* **1970**, *92*, 5118.
(40) Julia, S.; del Mazo, J. M.; Avilla, L.; Elguero, J. *Org. Prep. Proc. Int.* **1984**, *16*, 299.
(41) Reger, D. L.; Grattan, T. C.; Brown, K. J.; Little, C. A.; Lamba, J. J. S.; Rheingold, A. L.; Sommer, R. D. *J. Organomet. Chem.* **2000**, *607*, 120.

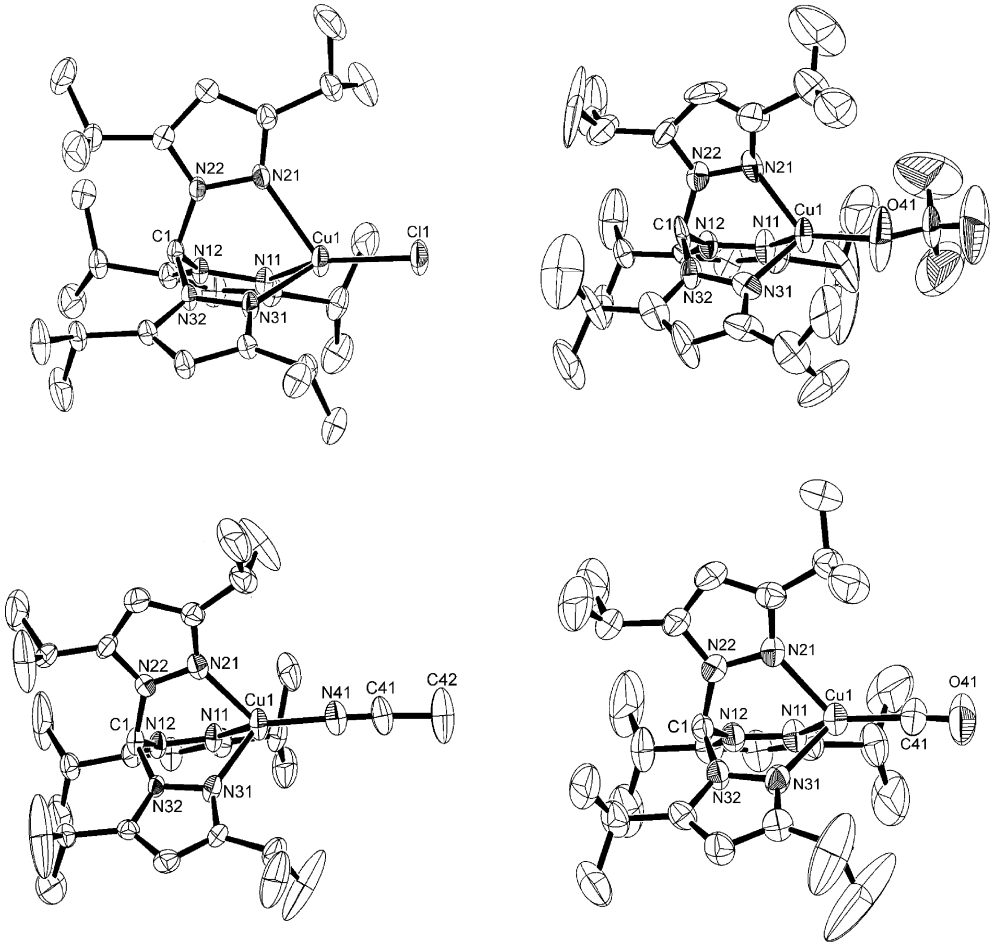

Figure 1. Crystal structures of [Cu(L1′)Cl] (**1**) (top left), [Cu(L1′)($OClO_3$)] (**2**) (top right), [Cu(L1′)(NCMe)]$^+$ (**3a**) (bottom left), and [Cu(L1′)(CO)]$^+$ (**4a**) (bottom right).

noncoordinating solvents. Complexes **4a** and **4b** were obtained from the reaction of **3a** and **2** with CO, respectively. [Cu(L3′)Cl] (**5**) and [Cu(L3′)(NCMe)](PF_6) (**6**) were prepared using ligand L3′. Note that complexes **5** and **6** were synthesized in the same manner as complexes **1** and **3a**, respectively. [Cu(L1)(NCMe)] (**7**) and [Cu(L1)(CO)] (**8**) were prepared using the borate ligand L1$^-$ and methods similar to those used for **3a** and **4a**, respectively. However, complex **7** is extremely sensitive toward O_2 in comparison to **3a** and **3b**. Finally, [Cu(L3)(NCMe)] (**9**) and [Cu(L3)-(CO)] (**10**) were synthesized using the borate ligand L3$^-$ in a manner similar to that used for complexes **7** and **8**, respectively. All procedures are described in detail in the Experimental Section and Supporting Information.

Structures. The newly prepared N3 type ligands L1′ and L3′ were obtained as suitable crystals, and their structures were determined by X-ray crystallography. The perspective drawings of L1′ and L3′ are shown in Figure S1, and their selected bond distances and angles are listed in Table S1. From the crystal structure, it is confirmed that the substituents at the third position of the pyrazolyl rings in L3′ are *t*Bu groups. Despite the different substituents, the average bond distances and angles are identical in L1′ and L3′. From these results, it becomes clear that the substituent at the third position of the pyrazolyl ring does not affect the ligand structures at all. Moreover, these structural parameters are also in close agreement with those of tris(pyrazol-1-yl)-methane[42a] and tris(3,5-dimethyl-1-pyrazolyl)methane.[42b] Importantly, though, in the resulting complexes derived from these ligands, differences in certain bond distances and angles are observed, which reflects the effect of the steric hindrance of the substituents in the complexes.

Complexes **1**, **2**, **3a**, **3b**, **4a**, **4b**, **5**, **6**, **7**, and **10** were also obtained as single crystals and investigated by X-ray crystallography, indicating that all complexes are mononuclear. The perspective drawings of their structures are shown in Figures 2 (**1**, **2**, **3a**, and **4a**), 3 (**5**, **6**, **7**, and **10**), and S2 (**3b** and **4b**). The selected bond distances and angles are listed in Tables S2 and S3.

In the copper(I) chloro complexes **1** and **5**, the copper(I) ions are tetrahedrally coordinated by three nitrogen atoms of L1′ and L3′, respectively, and one Cl$^-$ ligand. The Cu−Cl distance in **1** (2.181(1) Å) is slightly shorter than that in **5** (2.199(1) Å).

In the copper(I) perchlorato complex **2**, the copper(I) center is tetrahedrally coordinated by three nitrogen atoms of L1′ and one oxygen atom of the perchlorate anion. The average Cu−N_{pz} distance for the tridentate ligand is 2.07(2) Å, whereas the Cu−O distance of 1.93(1) Å is slightly shorter.

(42) (a) McLauchlan, C. C.; Varda, A. N.; Giles, J. R. *Acta Crystallogr., Sect. E.* **2004**, *60*, o1419. (b) Declercq, J.-P.; Meerssche, M. V. *Acta Crystallogr., Sect. C.* **1984**, *40*, 1098.

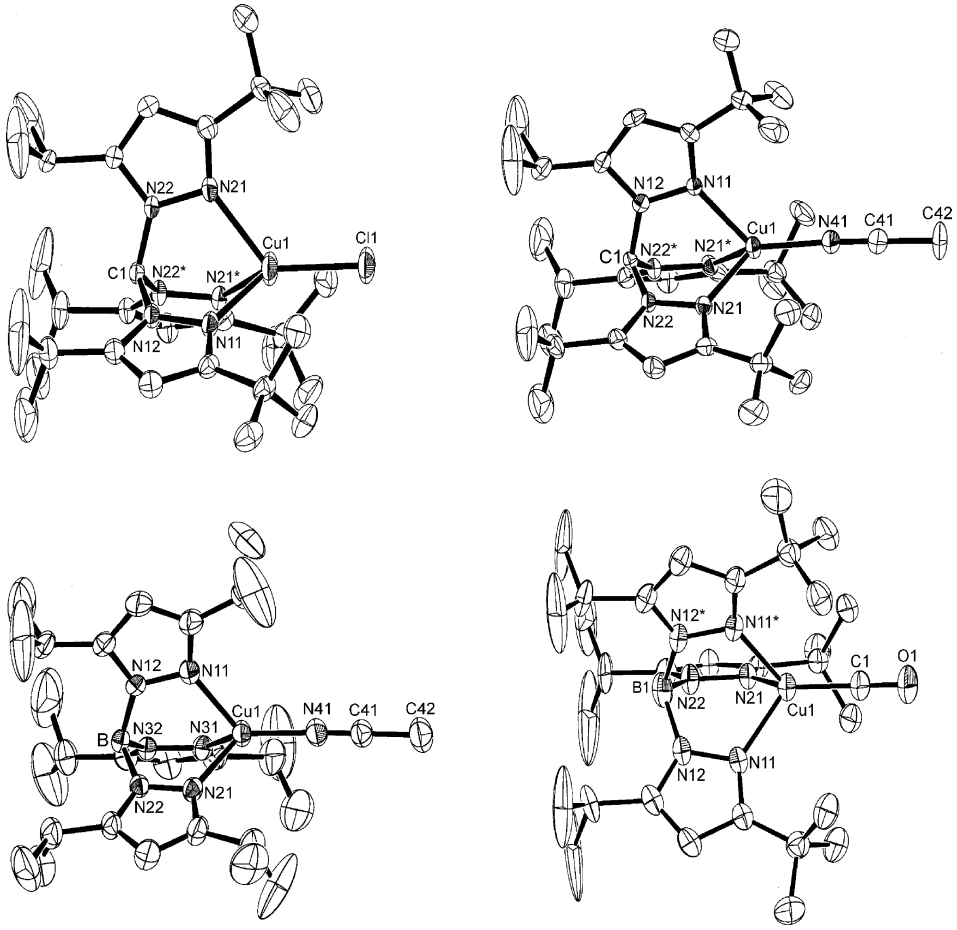

Figure 2. Crystal structures of [Cu(L3′)Cl] (**5**) (top left), [Cu(L3′)(NCMe)]$^+$ (**6**) (top right), [Cu(L1)(NCMe)] (**7**) (bottom left), and [Cu(L3)(CO)] (**10**) (bottom right).

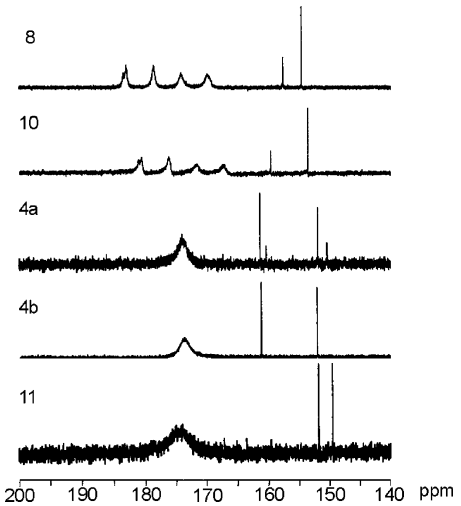

Figure 3. ^{13}C NMR spectra of copper(I) carbonyl complexes: [Cu(L1)(CO)] (**8**), [Cu(L3)(CO)] (**10**), [Cu(L1′)(CO)](PF$_6$) (**4a**), [Cu(L1′)(CO)](ClO$_4$) (**4b**), and [Cu(L5)(CO)] (**11**).

In the copper(I) acetonitrile complexes **3a**, **3b**, **6**, and **7**, the copper(I) ions are tetrahedrally coordinated by three nitrogen atoms of L1′ (**3a** and **3b**), L3′ (**6**), or L1$^-$ (**7**) and one nitrogen atom of acetonitrile. The copper(I) ions are almost linearly ligated by acetonitrile in all cases (Cu−N−C angle = 176−179°; Tables S2 and S3). The Cu−N distances to the nitrogen atom of acetonitrile are almost identical in these complexes (i.e., 1.887(5) Å for **3a**, 1.864(6) Å for **3b**, 1.883(3) Å for **6**, and 1.875(6) Å for **7**). The geometric parameters of the reported complex [Cu{HC(3-*t*Bupz)$_3$}(NCMe)](PF$_6$)[20] are similar to those of **6**, whose substituents at the third position of the pyrazolyl rings are also *t*Bu. This implies that the steric hindrance at the third position of the pyrazolyl rings does not significantly affect the structures of the acetonitrile complexes because this ligand is not very space demanding.

Finally, the copper(I) carbonyl complexes **4a**, **4b**, and **10** also show tetrahedral coordination polyhedra, where three nitrogen atoms of L1′ (**4a** and **4b**) or L3$^-$ (**10**) and one carbon atom of carbon monoxide are bound to the copper(I) ion. In **4a**, **4b**, **10**, and in the already reported complexes **8** and **11** ([Cu(L5)(CO)]),[13,14b,15] the copper(I) ions are almost linearly ligated by carbon monoxide with Cu−C−O angles in the range of 176−180° (Tables S2 and S3). The Cu−C distances are 1.783(7) Å for **4a**, 1.777(5) Å for **4b**, 1.769(8) Å for **8**, 1.76(1) Å for **10**, and 1.78(1) Å for **11**. Hence, the Cu−C distances of **4a**, **4b** with L1′, and **11** with L5$^-$ are quite similar. Importantly, the Cu−C bond length of **8** with L1$^-$ is relatively shorter than that in complexes with the corresponding methane ligand (**4a** and **4b**). This indicates a significant difference in the properties of borate and methane complexes with *identical* pyrazolyl substituents. Hence, these differences must then relate to the total charge of the ligands. This is also evident from a comparison of the structural

Table 3. Selected Structural Parameters for Copper(I) Carbonyl Complexes Ligated by Borate or Methane Ligands

	Cu−N (av) (Å)	Cu−C (Å)	C−O (Å)	N−Cu−N (av) (deg)	N−Cu−C (av) (deg)	Cu−C−O (deg)	ref
[Cu{HC(3,5-*i*Pr$_2$pz)$_3$}(CO)](PF$_6$) (**4a**)	2.053(11)	1.783(7)	1.118(9)	88.1(7)	126.6(3)	175.6(6)	this work
[Cu{HC(3,5-*i*Pr$_2$pz)$_3$}(CO)](ClO$_4$) (**4b**)	2.041(10)	1.777(5)	1.127(6)	87.9(14)	126.7(3)	176.7(5)	this work
[Cu{HB(3,5-*i*Pr$_2$pz)$_3$}(CO)] (**8**)	2.018(4)	1.769(8)	1.118(10)	90.8(9)	124.7(4)	178.6(9)	13b,14,15
[Cu{HB(3-*t*Bu-5-*i*Prpz)$_3$}(CO)] (**10**)	2.059(1)	1.76(1)	1.14(1)	92.9(8)	123.2(2)	178(1)	this work
[Cu{HB(3,5-Ph$_2$)$_3$}(CO)] (**11**)	2.059(6)	1.78(1)	1.08(1)	90.4(2)	125.0(2)	180.0(1)	13b, 14, 15
[Cu{HC(3-*t*Bupz)$_3$}(CO)](PF$_6$)	2.080(7)	1.778(10)	1.133(9)	89.0(28)	126.0(27)	176.8(9)	20
[Cu{HB(pz)$_3$}(CO)]	2.047(7)	1.765(11)	1.120(13)	91.3(5)	124.4(25)	178(2)	11, 12
[Cu{HB(3-*t*Bu-5-Mepz)$_3$}(CO)]	2.062(5)	1.797(11)	1.110(6)	92.7(9)	123.3(18)	177.6(8)	15, 16
[Cu{HB(3-CF$_3$pz)$_3$}(CO)]	2.052(11)	1.790(4)	1.126(5)	90.6(9)	124.8(9)	179.0(4)	18
[Cu{HB(3-C$_2$F$_5$pz)$_3$}(CO)]	2.075(11)	1.804(4)	1.115(5)	90.6(3)	124.9(21)	178.1(4)	19
[Cu{HB(3-C$_3$F$_7$pz)$_3$}(CO)]	2.078(7)	1.799(10)	1.119(13)	90.4(19)	125.0(32)	178.7(6)	19
[Cu{HB(3,5-(CF$_3$)$_2$pz)$_3$}(CO)]	2.052(15)	1.808(4)	1.110(5)	90.0(4)	125.3(7)	179.8(4)	17

parameters of [Cu{HC(3-*t*Bupz)$_3$}(CO)](PF$_6$)[20] from the literature with the borate complex [Cu(L3)(CO)] (**10**). Again, the borate complex exhibits shorter Cu−CO distances indicating a somewhat stronger Cu−C bond in this case. On the other hand, the Cu−C bond lengths in [Cu{HC(3-*t*Bupz)$_3$}(CO)](PF$_6$) and **4a** and **4b** with the methane ligand L1′ are identical, which shows that the effect of steric hindrance is negligible for the small CO ligand. The structure of the published complex [Cu{HB(3-*t*Bu-5-Mepz)$_3$}(CO)][15,16] is considerably similar to that of **10** with ligand L3$^-$, where the substituents at the third position of the pyrazolyl rings are, in both cases, *t*Bu. The comparison of borate ligand complexes with different alkyl substituents at the fifth position of the pyrazolyl rings again shows similar structures. This allows for two important conclusions: *the substituents at the third and especially the fifth position only play a minor role for the structures of the carbonyl complexes*. On the other hand, *the overall charge of the ligand significantly influences the properties of the Cu−C bond*. Note that the C−O bond distances are very similar in all complexes with exception of **11**, where a somewhat shorter distance is observed. The selected bond distances and angles of all structurally characterized carbonyl complexes are summarized in Table 3.

General Spectroscopic Characterization of the Complexes. ^{1}H and ^{13}C NMR spectra were measured for both ligands, L1′ and L3′, and for all the obtained complexes. In all cases, appropriate signals of the protons and carbon atoms of the N3 type ligands are observed. In L1′ and L3′ and all complexes with these ligands, the singlet signal of the CH proton is found, confirming the presence of a methane type ligand. L1′ and L3′ show this signal at 8.27 ppm. In comparison, this peak is shifted upfield in all complexes. On the other hand, the signal of the BH proton in borate type ligands and all corresponding complexes is not observed experimentally, which is the common case.[8−10,13−19]

In the carbonyl complexes, the signal of the carbonyl carbon atom can be detected by ^{13}C NMR spectroscopy. In general, ^{13}C NMR resonances for the terminal CO ligands in classical metal carbonyls appear in the range of 184−223 ppm.[43] On the other hand, terminal CO ligands in nonclassical metal carbonyls show relatively lower chemical shifts in the range of 140−189 ppm.[43] The complexes prepared in this study using unlabeled CO do not show any signals of the carbonyl carbon atom because of the low abundance of ^{13}CO in nature. Therefore, the carbonyl complexes were prepared using ^{13}C-enriched carbon monoxide. Using the labeled compounds of **4a** and **4b**, broad signals of the carbonyl carbon atoms are observed at 174.0 and 173.7 ppm, respectively (Figure 3 and Table 4). On the other hand, the ^{13}C NMR signals of the carbonyl carbons appear to be split into four broad peaks in **8** and **10**, observed at av 176.4 ppm (Δav 657 Hz) and av 174.0 ppm (Δav 655 Hz), respectively. For comparison, the previously reported carbonyl complex [Cu{HB(3,5-Ph$_2$pz$_3$)}(CO)] (**11**) shows only one broad ^{13}C-signal at 173.8 ppm. Importantly, the observation of a split ^{13}C carbonyl resonance has never been reported before for either copper(I) borate or methane complexes or analogous compounds using bidentate "N2" ligands to our knowledge.[11−19,44−46]

Table 4. ^{13}C Chemical Shifts of Copper(I) Carbonyl Complexes

	δ(^{13}C) (ppm)	average (ppm)
[Cu(L1)(CO)] (**8**)	169.9, 174.1, 178.7, 183.0	176.4
[Cu(L3)(CO)] (**10**)	167.5, 171.7, 176.3, 180.6	174.0
[Cu(L1′)(CO)](PF$_6$) (**4a**)	174.0	
[Cu(L1′)(CO)](ClO$_4$) (**4b**)	173.7	
[Cu(L5)(CO)] (**11**)	173.8	

In the acetonitrile complexes **3a**, **3b**, **6**, **7**, and **9**, the broad signals of the acetonitrile protons are observed in the ^{1}H NMR spectra at ca. 2.3 ppm, showing in each case an integrated intensity equivalent to 3 protons. However, the ^{13}C signals of the acetonitrile carbons could not be detected except for **7**, which is because they are usually strongly broadened.[20,46]

IR and far-IR spectra of all complexes were measured using KBr and CsI pellets, respectively. In KL1, KL3, KL5, and all corresponding complexes with these N3-type ligands, absorption bands of the B−H stretching vibration ν(B−H) are observed. For the free ligands, bands at 2467 (KL1),[14] 2469 (KL3),[15] and 2527 cm^{-1} (KL5)[14] are assigned to this

(43) (a) Abuke, F.; Wang, C. *Coord. Chem. Rev.* **1994**, *137*, 483. (b) Weber, L. *Angew. Chem., Int. Ed. Engl.* **1994**, *33*, 1077. (c) Willner, H.; Abuke, F. *Angew. Chem., Int. Ed. Engl.* **1997**, *36*, 2402. (d) Strauss, S. H. *J. Chem. Soc., Dalton Trans.* **2000**, 1. (e) Lupinetti, A. J.; Strauss, S. H.; Frenking, G. *Prog. Inorg. Chem.* **2001**, *49*, 1.
(44) (a) Dias, H. V. R.; Jin, W. *J. Am. Chem. Soc.* **1995**, *117*, 11381. (b) Dias, H. V. R.; Wang, Z.; Jin, W. *Inorg. Chem.* **1997**, *36*, 6205.
(45) Dias, H. V. R.; Jin, W. *Inorg. Chem.* **1996**, *35*, 3687.
(46) Dias, H. V. R.; Singh, S. *Inorg. Chem.* **2004**, *43*, 5786.

Table 5. Carbonyl Stretching Frequencies for Copper(I) Carbonyl Complexes and Copper(I) Containing Proteins

	νCO (cm^{-1})	ref
[Cu{HC(3,5-*i*Pr$_2$pz)$_3$}(CO)](PF$_6$) (**4a**)	2107	this work
[Cu{HC(3,5-*i*Pr$_2$pz)$_3$}(CO)](ClO$_4$) (**4b**)	2107	this work
[Cu{HB(3,5-*i*Pr$_2$pz)$_3$}(CO)] (**8**)	2056	this work, 13b, 14, 15
[Cu{HB(3-*t*Bu-5-*i*Prpz)$_3$}(CO)] (**10**)	2057	this work, 15
[Cu{HB(3,5-Ph$_2$pz)$_3$}(CO)] (**11**)	2080	this work, 13b, 14, 15
CO (free)	2143	44, 47, 48
[Cu{HC(3,5-Me$_2$pz)$_3$}(CO)](PF$_6$)	2113	19
[Cu{HC(3-Phpz)$_3$}(CO)](PF$_6$)	2104	19
[Cu{HC(3-*t*Bupz)$_3$}(CO)](PF$_6$)	2100	19
[Cu{HB(pz)$_3$}(CO)]	2083	11
[Cu{HB(3,5-Me$_2$pz)$_3$}(CO)]	2066	11, 49
[Cu{HB(3-*t*Bupz)$_3$}(CO)]	2069	50
[Cu{HB(3-*t*Bu-5-Mepz)$_3$}(CO)]	2061	15, 16
[Cu{HB(3,4,5-Br$_3$pz)$_3$}(CO)]	2110	51
[Cu{HB(3-CF$_3$pz)$_3$}(CO)]	2100	18
[Cu{HB(3-C$_2$F$_5$pz)$_3$}(CO)]	2110	19
[Cu{HB(3-C$_3$F$_7$pz)$_3$}(CO)]	2102	19
[Cu{HB(3,5-(CF$_3$)$_2$pz)$_3$}(CO)]	2137	17
hemocyanin	2043−2063	52
nitrite reductase	2050	53
amine oxidase	2064−2085	54
peptidylglycine α-hydroxylating monooxygenase	2093	55
dopamine β-hydroxylase	2089	56
cytochrome oxidase	2038−2065	5f, 57

mode. In comparison, the B−H vibrations are shifted to higher energy in the complexes.

Vibrational Spectroscopic Characterization of the Carbonyl and Chloro Complexes. The copper(I) carbonyl complexes prepared in this study exhibit intense C−O stretching vibrations in the 2050−2100 cm^{-1} IR region and weak Cu−CO stretching vibrations in the far-IR spectra (Figures 4 and S3−S7). The Cu−C stretching vibrations ν(Cu−CO) are identified using ^{13}C-isotope labeling. All copper(I) carbonyl complexes discussed here exhibit one isotope-sensitive signal around 450 cm^{-1} that is therefore assigned to this mode. Observed ^{13}C shifts are about 50 cm^{-1} for ν(C−O) and about 5 cm^{-1} for ν(Cu−CO).

The C−O stretching frequencies of the copper(I) carbonyl complexes with N3-type borate and methane ligands are listed in Table 5 in comparison to the values obtained for copper(I) carbonyl adducts in proteins. Importantly, a comparison of the different model complexes leads to the identification of a number of interesting trends for the C−O stretch. First, ν(C−O) is about 50 cm^{-1} higher in energy for the methane complexes compared to the borate complexes where the ligands have the same pyrazolyl substituents. Second, electron-donating substituents such as the *i*Pr or *t*Bu groups lead to lower ν(C−O) frequencies compared to methyl or aryl substituents in both the methane and borate complexes.[11,13−16,19,20,49−51] Vice versa, borate ligands containing halogenated substituents show ν(C−O) at higher energy than borate ligands containing aryl or methyl side chains. This leads to the following order in ν(C−O) frequencies for the pyrazolyl substituents in the borate ligands

$$i\mathrm{Pr}_2 \approx (t\mathrm{Bu}, i\mathrm{Pr}) < (t\mathrm{Bu}, \mathrm{Me}) < \mathrm{Me}_2 < (t\mathrm{Bu}, \mathrm{H}) < \mathrm{Ph}_2 < \mathrm{H}_2 < (\mathrm{CF}_3, \mathrm{H}) < \mathrm{Br}_3 < (\mathrm{CF}_3)_2 \quad (3)$$

Hence, it is possible, using halogenated pyrazolyl substituents, to shift ν(C−O) in borate complexes into the energy region normally only observed for methane complexes (>2100 cm^{-1}). These results indicate that *there is an important effect of the total charge of the N3 ligands and of the nature of the substituents on the electronic structures of the complexes*. The latter effect is of electronic and not steric origin for the carbonyl complexes. These tendencies observed experimentally are consistent with our DFT results (vide infra). Interestingly, the ν(C−O) frequencies of the copper(I) carbonyls in proteins are closer to the values obtained for the borate complexes compared to those obtained for the methane complexes (with alkyl substituents).[5f,52−57] This is surprising considering that the coordination environment of the type-2 copper center, for example in copper nitrite reductase, consists of three histidine ligands, which would correspond to a neutral methane ligand.

Another characteristic feature observed in the vibrational (far-IR) spectra of copper(I) chloro complexes is the Cu−Cl stretching vibration, which is found at 298 and 284 cm^{-1} in **1** and **5**, respectively (Figure S8). There is a 14 cm^{-1} difference between these two complexes in accordance with the differences in bond distances.

Electrochemical Studies of the Acetonitrile Complexes. To further explore the electronic effects of borate versus methane ligands, cyclic voltammetry measurements were performed on the copper(I) acetonitrile complexes **3a**, **6**, **7**, and **9** as shown in Figure 5. The data are summarized in Table 6. Only complex **9** shows a reversible redox process under the applied experimental conditions. This implies that the large substituents (*t*Bu and *i*Pr) probably hinder rearrangements of the complex upon oxidation. The other complexes show quasi-reversible redox behavior. We believe that dissociation of MeCN upon oxidation and a subsequent (undefined) structural rearrangement occurs, which is ultimately responsible for the quasi-reversible redox behavior even in MeCN solution. Importantly, it has been shown that the copper(I) acetonitrile complex ([Cu{HB(3-*t*Bupz)$_3$}(NCMe)]) exhibits a reversible redox behavior in CH_2Cl_2 solution after the addition of some MeCN,[58] which is in agreement with our results. This indicates that the complexes

(47) Braterman, P. S. *Metal Carbonyl Spectra*, Academic Press: New York, 1975.
(48) Nakamoto, K. *Infrared and Raman Spectra of Inorganic and Coordination Compounds*, 5th ed.; John Wiley & Sons: New York, 1997.
(49) Mealli, C.; Arcus, C. S.; Wilkinson, J. L.; Marks, T. J.; Ibers, J. A. *J. Am. Chem. Soc.* **1976**, *98*, 711.
(50) Ruggiero, C. E.; Carrier, S. M.; Antholine, W. E.; Whittaker, J. W.; Cramer, C. J.; Tolman, W. B. *J. Am. Chem. Soc.* **1993**, *115*, 11285.
(51) Caballero, A.; Díaz-Requejo, M. M.; Belderraín, T. R.; Nicasio, M. C.; Trofimenko, S.; Pérez, P. J. *J. Am. Chem. Soc.* **2003**, *125*, 1446.
(52) Fager, L. Y.; Alben, J. O. *Biochemistry* **1972**, *11*, 4786.
(53) Zhang, H.; Boulanger, M. J.; Mauk, A. G.; Murphy, M. E. P. *J. Phys. Chem. B.* **2000**, *104*, 10738.
(54) Hirota, S.; Iwamoto, T.; Tanizawa, K.; Adachi, O.; Yamauchi, O. *Biochemistry* **1999**, *38*, 14256.
(55) (a) Boswell, J. S.; Reedy, B. J.; Kulathila, R.; Merkler, D.; Blackburn, N. J. *Biochemistry* **1996**, *35*, 12241. (b) Jaron, S.; Blackburn, N. J. *Biochemistry* **1999**, *38*, 15086.

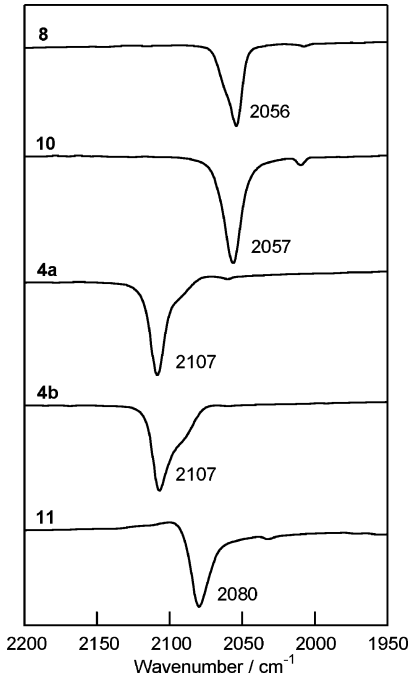

Figure 4. IR spectra of copper(I) carbonyl complexes: [Cu(L1)(CO)] (**8**), [Cu(L3)(CO)] (**10**), [Cu(L1′)(CO)](PF_6) (**4a**), [Cu(L1′)(CO)](ClO_4) (**4b**), and [Cu(L5)(CO)] (**11**).

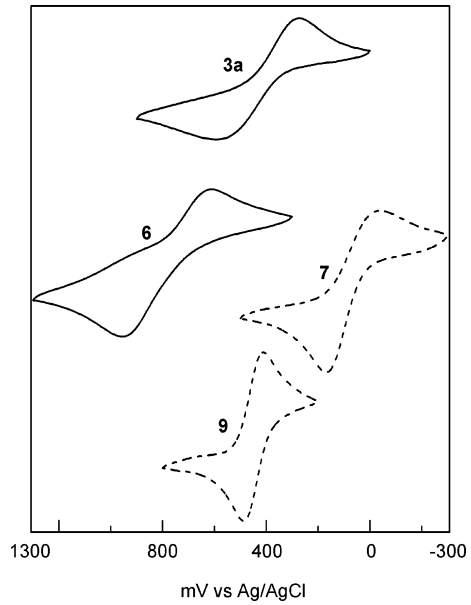

Figure 5. Cyclic voltammograms of the copper(I) acetonitrile complexes with methane ligands (—) (**3a** and **6**) and borate ligands (- - -) (**7** and **9**).

3a, **6**, and **7** are unable to keep their tetrahedral geometry after oxidation to copper(II) even in MeCN solution. The E_{pa} values of all complexes are gradually shifted to higher potentials in the following order: **7** (173 mV) ≪ **9** (483 mV) < **3a** (577 mV) ≪ **6** (936 mV). These results indicate some interesting tendencies: (1) the redox potentials of borate complexes are less than those of methane complexes with identical pyrazolyl substituents, and (2) the redox potentials of complexes with (3,5-*i*Pr$_2$)-substituted ligands are less than those of (3-*i*Pr, 5-*t*Bu)-substituted ligands. Of these complexes, **7** has the lowest oxidation potential, and correspondingly, only this compound reacts easily with O_2 to yield the μ-η^2:η^2 peroxo complex (vide infra). The formation of the corresponding peroxo complexes is much slower for **3a** and **3b**. In the case of **9**, the corresponding O_2 adduct, [Cu(L3)-(O_2)], could not be obtained.[59] Therefore, the ligands L1′ and L3$^-$ require different copper(I) starting materials to induce reactivity with O_2.[29,60]

Table 6. Results of Cyclic Voltammetry Experiments on Solutions of Copper(I) Acetonitrile Complexes[a]

complex	E_{pa} (mV)	E_{pc} (mV)	$E_{1/2}$ (mV)[b]	ΔE (mV)[c]
[Cu(L1′)(NCMe)](PF_6) (**3a**)	577	284	qr[d]	293
[Cu(L3′)(NCMe)](PF_6) (**6**)	936	634	qr[d]	302
[Cu(L1)(NCMe)] (**7**)	173	−35	qr[d]	208
[Cu(L3)(NCMe)] (**9**)	483	412	448	71

[a] Potentials are reported vs nonaqueous Ag/AgCl (see Experimental Section). [b] $E_{1/2} = (E_{pa} + E_{pc})/2$. [c] $\Delta E = E_{pa} - E_{pc}$. [d] qr means quasi-reversible.

Electronic Structure of the Carbonyl Complexes. To further investigate the electronic structure of the copper(I) carbonyl complexes and the influence of the total charge of the tripodal ligand on the properties of the Cu(I)-C−O unit, we performed DFT calculations. For these calculations, the corresponding 3,5-dimethyl substituted ligands, hydrotris-(3,5-dimethyl-1-pyrazolyl)borate (L0$^-$) and tris(3,5-dimethyl-1-pyrazolyl)methane (L0′), were used. Figure 6 shows the optimized structure of the borate complex [Cu(L0)(CO)] and Table 7 lists key structural parameters and calculated vibrational frequencies for this model. Calculated Cu−CO and averaged Cu−N_{pz} distances of 1.83 and 2.07 Å, respectively, show very good agreement with the experimental structure of [Cu(L1)(CO)]. In addition, the calculated C−O stretching frequency of 2008 cm^{-1} is in good agreement with the value of 2056 cm^{-1} obtained for [Cu(L1)-(CO)]. In all carbonyl complexes investigated in this paper, copper is in the oxidation state +I which corresponds to a d^{10} electron configuration of the metal. Hence, no donation from ligand orbitals into the d orbitals of copper is possible. Thus, the Cu(I)−CO interaction is entirely dominated by π back-bonding between the two degenerate π^* orbitals of CO and two t_2 type d orbitals of copper. This is confirmed by a detailed inspection of the MO diagram of [Cu(L0)(CO)]. Because of the distorted geometry of the complex, the occupied d orbitals are quite strongly mixed. Hence, the strength of the Cu−CO back-bond is easier to quantify from

(56) (a) Blackburn, N. J.; Pettingill, T. M.; Seagraves, K. S.; Shigeta, R. T. *J. Biol. Chem.* **1990**, *265*, 15383. (b) Pettingill, T. M.; Strange, R. W.; Blackburn, N. J. *J. Biol. Chem.* **1991**, *266*, 16996.
(57) (a) Alben, J. O.; Moh, P. P.; Fiamingo, F. G.; Altschuld, R. A. *Proc. Natl. Acad. Sci. U.S.A.* **1981**, *78*, 234. (b) Einarsdóttir, O.; Killough, P. M.; Fee, J. A.; Woodruff, W. H. *J. Biol. Chem.* **1989**, *264*, 2405. (c) Hill, J.; Goswitz, V. C.; Calhoun, M.; Garcia-Horsman, J. A.; Lemieux, L.; Alben, J. O.; Gennis, R. B. *Biochemistry* **1992**, *31*, 11435.
(58) Carrier, S. M.; Ruggiero, C. E.; Houser, R. P.; Tolman, W. B. *Inorg. Chem.* **1993**, *32*, 4889.
(59) Because of the bulky *t*Bu substituents in L3$^-$, corresponding copper(I) complexes are not able to form bridging (dinuclear) peroxo complexes. In this case, only mononuclear superoxo copper(II) complexes can be obtained.[60]
(60) (a) Fujisawa, K.; Tanaka, M.; Moro-oka, Y.; Kitajima, N. *J. Am. Chem. Soc.* **1994**, *116*, 12079. (b) Chen, P.; Root, D. E.; Campochiaro, C.; Fujisawa, K.; Solomon, E. I. *J. Am. Chem. Soc.* **2003**, *125*, 466.

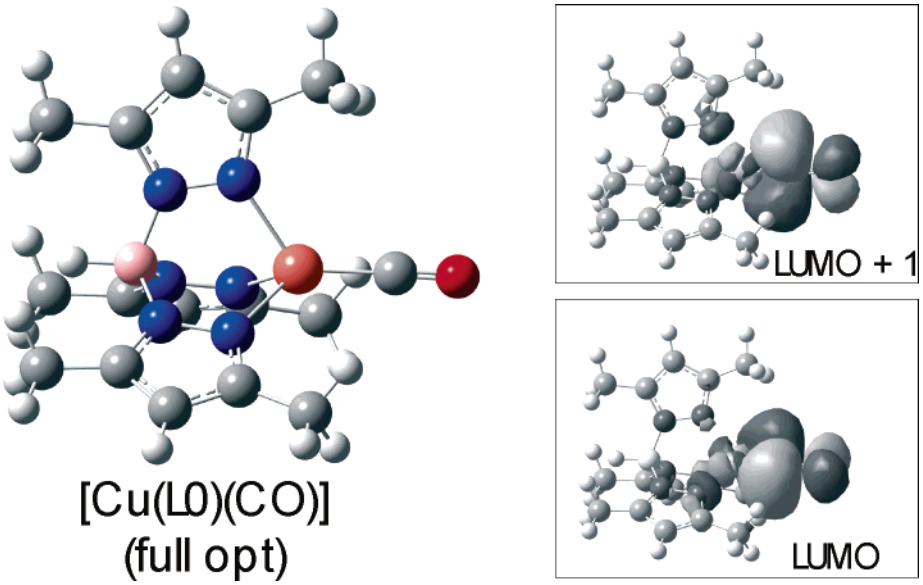

Figure 6. Fully optimized structure of [Cu(L0)(CO)] (left). Contour plots of important molecular orbitals of [Cu(L0)(CO)] illustrating the Cu(I)−CO back-bonding interaction (right). Calculated with BP86/TZVP.

Table 7. Comparison of the Calculated and Experimental Structures and Vibrational Frequencies of Copper(I) Carbonyl Adducts with Borate (L0$^-$, L1$^-$) and Methane (L0′, L1′) Tripodal Ligands

	geometric parameters (Å)			vibrational frequencies (cm^{-1})		
molecule/parameter	Δ(Cu−C)	Δ(C−O)	Δ(Cu−N_{pz})[a]	ν(C−O)	ν(Cu−CO)	δ(Cu−C−O)
[Cu(L0)(CO)]/DFT[b]	1.834	1.173	2.072	2008	445	352
[Cu(L1)(CO)]	1.77	1.12	2.02	2056	466	−
[Cu(L0′)(CO)]$^+$/DFT[b]	1.848	1.166	2.101	2056	432	343
[Cu(L1′)(CO)](PF_6)	1.78	1.12	2.053	2107	449	−
Δ(L0′ − L0)/DFT	+0.01	−0.01	0.03	48	−13	−9
Δ(L1′ − L1)/exptl	+0.01	∼0	0.03	51	−17	−

[a] Average of the three Cu−N_{pz} bond lengths. [b] Calculated with B3LYP/LanL2DZ; see Experimental Section.

the corresponding antibonding combinations ($\pi^*\_d_\pi$) between π^* of CO and the t_2 d orbitals of copper. These are shown in Figure 6 (right). Both have about 76% π^* and 13% d contribution, which corresponds to a medium strong back-bond. Because of the partial occupation of the π^* orbitals of CO that results from the back-bond, the strength of the C−O bond and hence the C−O stretching frequency should be sensitive to the total strength of the Cu(I)−CO interaction. This is confirmed by comparison of ν(C−O) for the corresponding borate and methane complexes, [Cu(L1)(CO)] and [Cu(L1′)(CO)](PF_6): as shown in Table 7, a shift of this vibration from 2056 in the borate to 2107 cm^{-1} in the methane complex is observed. This indicates a weakening of the Cu−CO back-bond in [Cu(L1′)(CO)](PF_6) compared to the back-bond in [Cu(L1)(CO)], which leads to a lower occupation of the CO π^* orbitals, and hence, a larger C−O stretching frequency in the methane complex. To further investigate this point, we have also fully optimized the structure of the methane complex [Cu(L0′)(CO)]$^+$. As shown in Table 7, good agreement between the calculated structural and vibrational properties of this system and the experimental data for [Cu(L1′)(CO)](PF_6) is obtained. As in the case of the borate system, the Cu−C distance obtained is slightly too long and ν(C−O) somewhat too low. However, the changes of the structural and vibrational parameters between the borate and methane systems (i.e., Δ(L′ − L)) are reproduced with excellent accuracy in the calculations as shown in Table 7 (bottom). Hence, on the basis of the calculations, the differences between these complexes can be analyzed quantitatively. Inspection of the MO diagram of [Cu(L0′)(CO)]$^+$ shows a small weakening of the Cu(I)−CO back-bond as compared to that of [Cu(L0)(CO)], which is evident from a lowered metal contribution of only 11% to the antibonding $\pi^*\_d_\pi$ orbitals. The slight weakening of the Cu−CO back-bond in the methane system then leads to an increase of ν(C−O) and a decrease of ν(Cu−CO) (i.e., a weakening of the Cu−CO bond and a strengthening of the C−O bond)[61] compared to those in the borate system. Importantly, the experimental data shows that the C−O stretching vibration is very sensitive to the extend of back-bonding and hence, in the case of the copper(I) complexes investigated here, can be used to probe the electron "richness" of the metal as a function of the employed N3 tripodal ligand. This leads to the conclusion that the methane ligands are weaker donors to copper(I) than the corresponding borate ligands, leading to an electron-poorer metal and hence

(61) Such an inverse correlation of the metal−C and the C−O stretching vibrations (and hence bond strengths) is typical for metal−ligand interactions that are dominated by back-bonding into ligand π^* orbitals. This has intensively been studied for [Fe^{II}(porphyrin)(CO)] complexes.[62]

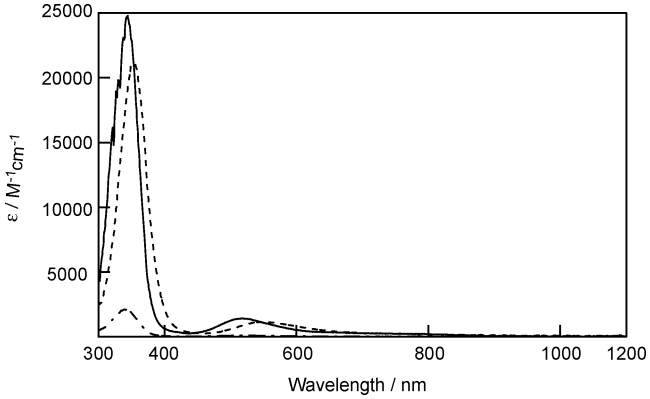

Figure 7. UV−vis spectra of the copper(II) peroxo complexes by the reaction of **2** (—), **3b** (-·-), and **7** (- - -) with O_2.

reduced back-donation to CO. This conclusion is in agreement with the electrochemical data presented above.

Reactivity. In this work, the reactivities of all prepared copper(I) complexes toward O_2 are also investigated. The absorption spectra of the products obtained by reaction of **2**, **3b**, and **7** with O_2 in dichloromethane at −80 °C are shown in Figure 7. For the L1′ complexes **2**, **3b**, and **4b**, perchlorate, acetonitrile, and carbon monoxide are present as the fourth ligand, respectively. Complex **2** shows a high reactivity toward O_2 as indicated by the immediate color change of the solution from colorless to deep purple upon addition of O_2. The absorption spectrum of the reaction mixture shows complete formation of the μ-η^2:η^2 peroxo complex, which has previously been characterized.[5d,5e,6,7,13,63] On the other hand, **3b** ligated by acetonitrile reacts slowly with O_2 as evidenced by a much slower color change of the solution as compared to **2**. After 701 h at −80 °C, only 8.6% conversion to the μ-η^2:η^2 peroxo complex was observed as indicated by the absorption spectrum of the reaction mixture. The same slow reaction of [Cu{HC(3,5-Me_2pz)$_3$}(NCMe)](PF_6) with O_2 has also been reported.[64] On the other hand, the copper(I) carbonyl complex **4b** does not react with O_2. In this case, only the starting material was recovered from the reaction mixtures.

The absorption spectra of the products obtained by the reaction of **3a** and **3b** with O_2 in dichloromethane at −80 °C are shown in Figures S9−S11. In both complexes, only the counteranion is different, which is PF_6^- in **3a** and ClO_4^- in **3b**. These absorption spectral changes indicate that the rate constants for the production of the corresponding peroxo complexes are slightly different because of the effect of the different counterions.[13,29] In comparison, the reactivity of borate complex **7**, which contains ligand L1$^-$ that carries the same substituents as L1′ (**3a** and **3b**), toward O_2 is very high. In addition to the ligand type (methane or borate), the bulkiness of the substituents is also of critical importance as shown by comparison of different borate complexes: whereas the acetonitrile complex **7** (ligand L1$^-$) is highly reactive toward O_2, the acetonitrile complex **9** with the bulkier L3$^-$ ligand does not react. These results are consistent with the E_{pa} values shown in Table 6 and Figure 5. Correspondingly, because of the very high redox potential, **6** (ligand L3′) does not react with O_2 either.

Scheme 2. Reaction Cycle between Complexes **3a** (or **3b**) and **4a** (or **4b**) and the Corresponding Peroxo Complex

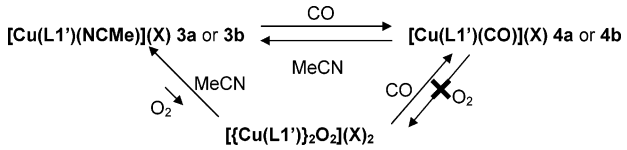

Scheme 3. Reaction Cycle between Complexes **7** and **8** and the Corresponding Peroxo Complex

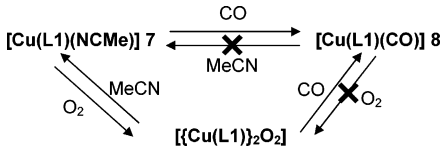

In Scheme 2, the reaction cycle between complexes **3a**, **4a**, and the corresponding peroxo complex is shown. The reaction of **3a** with CO corresponds to the procedure used for the synthesis of **4a**, which is reversible. The low reactivity of **3a** toward O_2 has already been discussed. Complex **4a** does not react with O_2 at all. The peroxo complex itself can be transformed back to **3a** or **4a** by dissolving it in acetonitrile or by reaction with CO in dichloromethane, respectively, which leads to a color change of the solution from purple to colorless. These reactions are observed for both counteranions, PF_6^- (**3a** and **4a**) and ClO_4^- (**3b** and **4b**).

In Scheme 3, the reaction cycle between **7**, **8**, and the corresponding peroxo complex is shown. The reaction of **7** with CO corresponds to the procedure used for the synthesis of **8**. In this case, this reaction is irreversible. The higher reactivity of **7** toward O_2 compared to **3a** and **3b** has already been discussed, whereas **8** does not react with O_2, in agreement with **4a** and **4b**. The peroxo complex can be transformed back to **7** or **8** by dissolving it in acetonitrile or by reaction with CO in solution, respectively, as revealed by spectroscopy. This means that complex **7** shows fully reversible binding of O_2. This is the common case for the other structurally characterized μ-η^2:η^2 peroxo complexes.[63] Moreover, this means that the μ-η^2:η^2 peroxo complex with L1$^-$, [{Cu[HB(3,5-*i*Pr_2pz)$_3$]}$_2$(μ-O_2)], is a good structural and functional model for oxy-hemocyanin.

Discussion

At first, the differences in the fourth ligand and the counteranion and their influence on the experimental properties of the complexes are discussed. In **2**, **3b**, and **4b**, the copper(I) ions are ligated by the neutral N3-type ligand L1′ with perchlorate, acetonitrile, and carbon monoxide as the fourth ligand (X), respectively. As shown in Figure 7, the reactivity toward O_2 varies dramatically depending on the nature of the fourth ligand. This is determined by the

(62) (a) Li, X.-Y.; Spiro, T. G. *J. Am. Chem. Soc.* **1988**, *110*, 6024. (b) Ray, G. B.; Li, X.-Y.; Ibers, J. A.; Sessler, J. L.; Spiro, T. G. *J. Am. Chem. Soc.* **1994**, *116*, 162 and references herein.
(63) (a) Kodera, M.; Katayama, K.; Tachi, Y.; Kano, K.; Hirota, S.; Fujinami, S.; Suzuki, M. *J. Am. Chem. Soc.* **1999**, *121*, 11006. (b) Kodera, M.; Kajita, Y.; Tachi, Y.; Katayama, K.; Kano, K.; Hirota, S.; Fujinami, S.; Suzuki, M. *Angew. Chem., Int. Ed.* **2004**, *43*, 334.
(64) Cvetkovic, M.; Batten, S. R.; Moubaraki, B.; Murray, K. S.; Spiccia, L. *Inorg. Chim. Acta* **2001**, *324*, 131.

coordinating atom, the strength of the resulting Cu(I)−X bond, and the size of X. Perchlorate ligates the copper(I) ion by an oxygen atom. The Cu(I)−$OClO_3$ bond is quite weak, which relates to perchlorate being in general a weak ligand, but it is also related to the large size of the perchlorate anion causing steric repulsion. As a result, a high reactivity of **2** toward O_2 is observed. On the other hand, acetonitrile in **3b** is coordinated by a nitrogen atom. The smaller size of acetonitrile causes less steric repulsion, resulting in lower reactivity toward O_2. In the carbonyl complex **4b**, the strongest Cu−X bond in this series of compounds is present with a calculated complex formation energy of about 33 kcal/mol. Hence, **4b** is inert toward O_2. Thus, it is clear that the fourth ligand strongly affects the reactivity of the complexes. Importantly, differences in the counteranion also seem to slightly affect the reactivity. Complexes **3a** and **3b** are both coordinated by the N3-type ligand L1′ and acetonitrile. However, they differ in the nature of the counteranion. As shown in Figures S9−S11, the reactivity toward O_2 is actually slightly different in these complexes, which relates to differences in the properties of the formed O_2 adducts in solution.[29]

Next, the effects of the total charge of the N3-type ligands on the structures, properties, and reactivities of the complexes are evaluated. In **3a** and **3b**, the neutral N3-type methane ligand (L1′) is present, whereas **7** is ligated by the corresponding anionic borate ligand ($L1^-$). All three compounds contain acetonitrile as a fourth ligand. Importantly, almost the same Cu−N (acetonitrile) bond distances are obtained for these complexes. However, their reactivities toward O_2 are clearly different, which must be related to the different total charges of the complexes and hence the different charges of the N3 ligands. While a neutral L1′ ligand forms cationic complexes with copper(I), the negatively charged $L1^-$ ligand forms a neutral complex. These differences are nicely reflected by the different redox potentials of **3a** and **7**: while **3a** has an oxidation potential of $E_{pa} = 577$ mV, this value is decreased to 173 mV in **7**. Therefore, the neutral methane ligands seem to donate less to the copper(I) center compared to the corresponding borate ligands, which leads to *an electron-poorer copper(I) in the methane complexes* and hence to an increased redox potential. As a consequence, the methane complexes show a lower reactivity toward the oxidant O_2. The redox potentials of complexes with the bulkier L3′ and $L3^-$ ligands, **6** and **9**, respectively, also reflect this trend. More insight into the differences between the methane and borate complexes is available by comparison of the corresponding carbonyl complexes. As evident from the DFT calculations, the Cu(I)−CO interaction in these systems is entirely dominated by back-bonding. Hence, the electron-poorer copper(I) centers in methane complexes should form weaker Cu−CO bonds as compared to those of the corresponding borate complexes with identical pyrazolyl substituents. This should lead to stronger Cu−C and weaker C−O bonds in the borate complexes as reflected by the corresponding bond lengths and vibrational frequencies. These predictions from the DFT calculations exactly match what is observed experimentally. The Cu−C bond distance is shorter in **8** (1.769(8) Å) with borate ligand $L1^-$ than those in **4a** (1.783(7) Å) and **4b** (1.777(5) Å) with methane ligand L1′. Correspondingly, the Cu−C stretching frequency in **8** (466 cm^{-1}) is higher than those in **4a** (449 cm^{-1}) and **4b** (447 cm^{-1}). Hence, the Cu−CO bond is indeed somewhat stronger in the borate complexes than it is in the methane complexes. The C−O stretching frequencies are also in full agreement with this trend: for **8**, a lower ν(C−O) of 2056 cm^{-1} is observed compared to those of **4a** (2107 cm^{-1}) and **4b** (2107 cm^{-1}), where ν(C−O) is shifted by ∼50 cm^{-1} to higher energy. These trends are also observed for all other pairs of corresponding methane and borate ligands (Table 5). Hence, the C−O stretching vibration is the most direct and most sensitive probe for the electron richness of copper(I) in these tripodal complexes. Since CO is a small ligand, its binding to copper(I) should not be influenced by steric effects from bulky pyrazolyl substituents. Therefore, the C−O stretching mode can also be used to generally classify the copper(I) borate and methane complexes with respect to the electronic richness or poorness of the copper(I) centers *independent of the steric nature of the N3 ligand used*. One interesting result from Table 5 is that by using halogenated substituents in borate complexes, C−O stretching frequencies in the range of the methane complexes (∼2100 cm^{-1}) can be obtained. This means that an electron poorness of the copper(I) center comparable to methane complexes can also be achieved in borate complexes by tuning the properties of the ligand. In contrast to the vibrational results, the ^{13}C NMR shifts of the carbonyl carbons do not show much sensitivity to the nature of the complexes. Interestingly, the ^{13}C signals of some complexes appear to be split because of coupling with the Cu nuclear spin of $I = 3/2$. To our knowledge, this has not been observed before for Cu(I)−CO complexes. The reason that this splitting only occurs for certain complexes is not clear.[65]

Finally, the effects of the steric hindrance at the third position of the pyrazolyl rings in N3-type ligands on the structures, properties, and reactivities of the complexes are discussed. Ligands L1′ and L3′ differ in the substituents at the third position of the pyrazolyl rings (L1′:*i*Pr; L3′:*t*Bu). This influences the bond lengths between copper(I) and the coordinated fourth ligands. In the case of the corresponding chloro complexes, the Cu−Cl distance for **5** (2.199(1) Å) with the bulkier ligand is elongated by 0.018 Å compared to that of **1** (2.181(1) Å). Correspondingly, **5** shows a lower Cu−Cl frequency (284 cm^{-1}) than **1** (298 cm^{-1}). Hence, the chloride anion experiences (stronger) steric repulsion in **5**, resulting in a weaker Cu−Cl bond. On the other hand, when acetonitrile is the fourth ligand, no such differentiation between L1′ (**3a**) and L3′ (**6**) is observed. Comparison of the carbonyl complexes with ligands L1′ (**4a**) and HC(3-*t*Bupz)$_3$ (Table 5) leads to a similar result. In these cases, the C−O stretching vibrations are observed at 2107 and 2100 cm^{-1}, respectively, indicating similar Cu(I)−CO bonds and hence negligible influences of the pyrazolyl substituents on the bonding of the small ligand CO. The reason for these

(65) We measured ^{13}C NMR of ^{13}C-enriched **4a** at low temperature (210 K). However, this broad peak was not split.

observations is straightforward: since both *i*Pr and *t*Bu groups have similar (donating) electronic effects on the pyrazolyl groups, L1′ and L3′ complexes only differ because of steric effects. Therefore, as might be expected, larger differences in the geometric and electronic structures of corresponding copper(I) complexes are only obtained for ligands that are at least of the size of the chloride anion, whereas for acetonitrile and CO, similar properties are found. A very similar situation is observed for the borate ligands. In complexes **8** and **10**, the copper(I) center is ligated by the $L1^-$ and $L3^-$ ligands, respectively, which carry *i*Pr ($L1^-$) and *t*Bu ($L3^-$) substituents at the third positions of the pyrazolyl rings. In both complexes, CO is the fourth ligand. Similar Cu−C distances (1.769(8) Å in **8** and 1.76(1) Å in **10**) and C−O stretching frequencies (2056 cm^{-1} in **8** and 2057 cm^{-1} in **10**) are observed for these compounds showing again that CO does not experience steric hindrances in these complexes and hence, similar Cu−CO bonds result. This again underlines the enormous significance of the carbonyl adducts, which selectively allow the electronic structure of the copper(I) center to be probed by simply determining ν(C−O). To further illustrate this point, let us consider the borate ligand with phenyl substituents in the third and fifth positions ($L5^-$). Importantly, while the alkyl groups are electron-donating substituents, the phenyl groups are electron-withdrawing groups leading to an electron-poorer copper(I) center. Indeed, this is proven by the carbonyl adduct of $L5^-$ (**11**), which has an elongated Cu−C bond (1.78(1) Å)[25] and a higher C−O stretching frequency (2080 cm^{-1}) compared to those of **8** and **10**, indicative of a weaker Cu−CO bond and hence an electron-poorer copper(I) in **11**. Although this analysis is sound and also in agreement with the DFT results, it leads to one important question: if the borate (or methane) complexes with *i*Pr and *t*Bu substituents have electronically similar copper(I) centers, then why are their oxidation potentials, E_{pa} (as given for the acetonitrile adducts in Table 6), so different? This difference in E_{pa} between **7** and **9**, for example (or **3a** and **6** for the corresponding methane ligands), is also manifested in the very different reactivities of these complexes toward O_2: while **7** reacts readily with O_2,[13] **9** does not.[60] However, oxidation of the copper(I) acetonitrile complexes to copper(II) is also coupled to a ligand exchange reaction as evident from the CV measurements showing only quasi-reversibility. Importantly, the reaction of O_2 also requires ligand exchange. Therefore, one possible explanation for the large difference in redox potentials and reactivities between **7** and **9** (or **3a** and **6**) is that the ligand exchange is unfavorable because of steric hindrance in the complexes with *t*Bu substituents. Alternatively, since the copper(I) centers are electronically similar in **7** and **9** (or **3a** and **6**), the observed differences must then relate to different stabilities of the formed copper(II) products. In general, the redox potential of a species relates to the difference in free energy ($\Delta G°$) of the oxidized and reduced forms. Hence, since the reduced copper(I) forms are similar in these complexes, the stabilities of the obtained copper(II) complexes must then be quite different depending on the steric hindrance of the applied N3 ligand to explain the shift in redox potentials. Experimental evidence that this is actually the case comes from the reaction of the free ligands $L1^-$ and $L3^-$ with copper(II) salts: while $L1^-$ easily forms copper(II) complexes, $L3^-$ does not. Hence, *the properties of the copper(II) complexes seem to be the determining factor for the differences in the redox properties of the copper(I) complexes with different pyrazolyl substituents*.

Conclusions

In this paper, copper(I) complexes ligated by N3-type ligands were systematically synthesized and characterized, and the reactivities of these complexes are described. Importantly, our results show that complexes with the neutral methane and anionic borate ligands differ in the electron richness of the copper(I) center, which is directly probed by the C−O stretching vibration in the corresponding carbonyl complexes. In fact, the borate ligands lead to more electron-rich copper(I) centers, in agreement with the observed redox potentials and reactivities of the complexes. The observed trends for different alkyl substituents of the pyrazolyl rings in these ligands are less clear. It is demonstrated, using CO as a probe, that the observed differences between the *i*Pr and *t*Bu-substituted ligands mostly relate to steric hindrance, whereas the electronic effect is negligible. Finally, the influence of the size and the nature of the fourth ligand are evaluated. On the basis of all of these results, it is possible to efficiently control the structures, electronic characters, and reactivities of four-coordinate copper(I) complexes by variation of the charge of the ligand, the degree of steric hindrance of the substituents, and the choice of the fourth ligand. In proteins, copper(I) centers are observed, which either react with O_2 or not, depending on their environment. Importantly, our results demonstrate how reactivity can be controlled by the structure and charge of the ligands. In this sense, the work presented here contributes to an understanding of how proteins are able to control the reactivities of "their" metal centers and how second coordination sphere effects contribute to this fine-tuning.

Acknowledgment. This research was supported in part by the Japan Society of the Promotion of Science (Grant-in-Aid for Scientific Research (B), Nos. 14350471 and 17350043) and by the Ministry of Education, Culture, Sports, Science and Technology (the 21st Century COE program (Promotion of Creative Interdisciplinary Materials Science for Novel Function)) to K.F. and the Fonds der Chemischen Industrie (FCI) to N.L.

Supporting Information Available: Syntheses of other complexes, crystal structures for L1′, L3′, **3b**, and **4b** (Figures S1 and S2), selected structural parameters (Tables S1−S3), IR and far-IR spectra of **4a**, **4b**, **8**, **10**, and **11** (Figures S3−S7), far-IR spectra of **1** and **5** (Figure S8), UV−vis absorption spectral changes (Figures S9−S11) and the corresponding data (Tables S4−S6) of **3a**, **3b**, and **7** at −78 °C. Crystallographic data are available in CIF format. This material is available free of charge via the Internet at http://pubs.acs.org. Crystallographic data have been deposited at the CCDC, 12 Union Road, Cambridge CB2 1EZ, UK and copies can be obtained on request, free of charge, by quoting the publication citation and the deposition numbers (278935−278946).

IC051290T